Finite Element Modelling of RC Beams Strengthened with Prestressed NSM CFRP Plate

by

Hamed Alfaidi

A thesis
presented to the University of Waterloo
in fulfillment of the
thesis requirement for the degree of
Master of Applied Science

in

Civil Engineering
Waterloo, Ontario, Canada, 2021

AUTHOR'S DECLARATION

I hereby declare that I am the sole author of this thesis. This is a true copy of the thesis, including any required final revisions, as accepted by my examiners.

I understand that my thesis may be made electronically available to the public.

Abstract

Near Surface mounted (NSM) carbon fibre reinforced polymer (CFRP) reinforcement has become a promising flexural strengthening technique for reinforced concrete (RC) elements. The prestressing of a CFRP plate can be used to provide RC members with further enhancements in the flexural capacity.

The aim of this study was to introduce a three-dimensional nonlinear finite element analysis (FEA) of RC beam strengthened by prestressed CFRP plate. Although there is a wide range of commercial programs for three-dimensional nonlinear FEA, they have different capabilities to model complex behaviour of composite materials such as RC beams strengthened with prestressed CFRP plate and the contact interaction. Therefore, the ABAQUS finite element package was used in this study due to its known accuracy to model the behaviour of a variety of materials such as concrete and its powerful contact algorithms. Concrete material was modelled using concrete damage plasticity (CDP) constitutive model, and steel reinforcements were modelled as elastic-perfectly plastic material. The CFRP plate was modelled as perfectly elastic material that fails at maximum tensile strain. Perfect bond was assumed between concrete and steel reinforcement, and a contact model was used to represent the behaviour between concrete and the CFRP plate.

The results of the FEA were validated against experiment results reported in the literature. The results were compared in terms of the load-deflection behaviour, crack patterns, and mode of failure (rupture or debonding of CFRP plate). Based on the validation, the proposed FEA model was capable of capturing the behaviour of RC beams strengthened with prestressed CFRP plate. A parametric study was conducted to investigate the effect of prestressing levels, steel grades, and thickness, width, and length of the CFRP plate. It was observed that increasing prestressing of the

CFRP plate improved the strength of the RC beam especially for the ultimate load. However, as the prestressing increased, the mode of failure changed to the rupture of the CFRP plate which limited further increase of the ultimate load. Using a higher steel grade improved the load carrying capacity. Increasing the width of the CFRP plate improved the load carrying capacity by delaying the debonding at the CFRP-concrete interface. Increasing CFRP plate thickness further improved the load carrying capacity of the beam. Increasing the length of the CFRP plate developed the general load carrying capacity; however, it was found that covering 25% of the shear span of RC beams provided sufficient and cost effective strengthening. The FE model offers a reasonable representation of the experimental results for load-deflection curve, failure modes and crack patterns.

Acknowledgements

First, I would like to thank and praise Allah for helping and guiding me to complete this work. I would like to express my sincere appreciation and gratitude to my parents and family for their unconditional love, support, helping and encouraging me throughout my life. This work would not be accomplished with out their praying, encouraging and I owe them the endless gratitude that I would never be able to pay back.

I also would like to acknowledge my supervisor Prof. Adil Al-Mayah. Prof. Al-Mayah has not only provided me with support and guidance during the master's program in both courses and research but has also implemented in me the importance of expanding my knowledge to new perspectives in the academic field that is important for growing future academic collaboration. Due to his kindness, humbleness, positive attitude when I was faced with difficulties in the research, he worked with me as a friend in a team more than a supervisor. Prof. Al-Mayah has shown me his great understanding and support in difficult times such as COVID 19 global pandemic.

I also would like to thank my reviewers Prof. Scott Walbridge, and Prof. Neil Thomson for their time that spent to review my thesis.

I also would like to thank Prof. Abdulwahab M. Zughaibi for his encouragement and being a role model for me in civil engineering since I was an undergrads student.

I also would like to thank Prof. Hassan Baaj for developing the idea, reviewing, and helping with published research paper about asphalt material properties. Without his contribution the research paper would take longer time to be accepted.

I also would like to especially thank my best friend Dr. Abdullah Kaki for his great wishes, and always offering me his assistance and support when needed.

I also would like to especially thank my friend Abdullah AlBiladi for his encouraging and his wide knowledge on the research which helped me in this study. Especial thanks to my friend Mustafa Alhusain

for sharing his great knowledge in the FRP reinforcement and its application in civil engineering, and his guiding in ABAQUS which that resulted on the success of this thesis.

I am also grateful to King Abdulaziz University, Saudi Arabia for fully sponsoring my scholarship and to Saudi Arabian Cultural Bureau in Canada for supporting throughout my study.

Extended thank to my friend: Dr. Amin Hamdi, Dr. Hani Eissa, Dr. Waleed Anber, Mousa Alhawsah, Abdulrahman Hamid, Ryan Barrage, and Graeme Milligan.

Dedication

I would like to dedicate this thesis to my parents.

Table of Contents

AUTHOR'S DECLARATION ii
Abstract iii
Acknowledgements v
Dedication vii
List of Figures x
List of Tables xii
Chapter 1: Introduction 1
1.1 General 1
1.2 Research Objective 3
1.3 Organization 4
Chapter 2: Literature Review 5
2.1 Introduction 5
2.2 Introduction to FRP 5
2.2.1 Fibres 7
2.2.2 Matrix 10
2.3 Bond between FRP Laminate and Concrete 10
2.4 FRP as Strengthening Materials for RC Members 12
2.5 Advantages and Disadvantage of Using FRP for Strengthening RC Members 13
2.5.1 Advantages of using FRP 13
2.5.2 Disadvantages of using FRP 13
2.6 Application of FRP in Civil Engineering 13
2.6.1 Introduction 13
2.6.2 Methods of using FRP in RC Members 14
2.6.3 Prestressing reinforcement on concrete 15
2.7 Failure Modes of RC Strengthened with FRP Laminate 16
2.8 Experimental Research on Strengthening Concrete with FRP 18
2.9 Numerical Research on Strengthening Concrete with FRP 22
2.10 Conclusion 26
Chapter 3: Development of Finite Element Model 27
3.1 Introduction 27
3.2 Model Configuration 28
3.3 Materials Modelling 29
3.3.1 Concrete 29

3.3.2 Steel 38
3.3.3 FRP Plate 40
3.4 Element Selection 41
3.4.1 Continuum or Solid Element 43
3.4.2 Truss Element 43
3.4.3 Shell Element 44
3.5 Contact between Elements 45
3.5.1 Contact between Concrete and Internal Reinforcement 46
3.5.2 Interface between Concrete and CFRP Plate 46
3.6 Prestressing of CFRP Plate 48
3.7 Boundary Conditions and Loading 51
3.8 Meshing 52
Chapter 4: Results and Validations 54
4.1 Introduction 54
4.2 Verification of Models for Behaviour of Control RC Beam 54
4.2.1 Dilation angle (ψ) 54
4.2.2 Viscoplastic regularization 56
4.2.3 Mesh refinement 57
4.3 Behaviour of Controlled RC Beam 58
4.4 Behaviour of RC Beam Strengthened with Non-prestressed CFRP Plate 60
4.5 Behaviour of RC Beam Strengthened by Prestressed CFRP Plate 63
4.5.1 Prestressing level of 5% 63
4.5.2 Prestressing level of 20% 65
4.5.3 Prestressing level of 30% 68
4.6 Comparison between FEM and Experimental Results for Yield Load 70
4.7 Comparison between FEM and Experimental Results for Ultimate Load 71
4.8 Recommendations for Modeling RC and Prestressed CFRP Plate 72
4.9 Conclusions 75
Chapter 5: Parametric Study 76
5.1 Introduction 76
5.2 Effect of Prestressing Level 76
5.3 Effect of Steel Strength 78
5.4 Effect of the Length of Prestressed CFRP Plate 81
5.5 Effect of the Width of Prestressed CFRP Plate 84
5.6 Effect of the Thickness of Prestressed CFRP Plate 86

5.7 Conclusion 89
Chapter 6: Conclusions and Recommendations 90
6.1 Introduction 90
6.2 Conclusions 90
6.3 Recommendations 91
Bibliography 93

List of Figures

Figure 2.1Schematic representation of a unidirectional composite (Reddy, 2003) 6
Figure 2.2 Tensile stress-strain behavior of various reinforcing fibres (ACI committee 440R, 1996)..... 7
Figure 2.3 Varying fibre orientation (reproduced from ACI committee 440R, 1996)..... 8
Figure 2.4 Strength relation to fibre orientation (reproduced from ACI committee 440R, 1996)..... 9
Figure 2.5 Tensile stress-strain relationships for the composite FRP and its components 10
Figure 2.6 Bilinear traction separation law (Burlayenko & Sadowski, 2008) 12
Figure 2.7Applications of FRP in civil engineering structures (van den Einde et al., 2003)..... 14
Figure 2.8 The effect of FRP prestressing level on RC beams performance (Yang et al., 2009) 15
Figure 2.9 Failure modes of RC beams strengthened with FRP laminates..... 17
Figure 3.1 Dimensions of experimental beam with CFRP plate (Hajihashemi, et al., 2011) 28
Figure 3.2 Parts of the FE model of the beam, steel reinforcement and stirrups and CFRP plate in ABAQUS 29
Figure 3.3 Compressive stress-strain relationship (ABAQUS Manual, 2011) 32
Figure 3.4 Compressive behaviour of concrete 35
Figure 3.5 Tensile stress-strain relationship (ABAQUS Manual, 2011) 36
Figure 3.6 Tensile behaviour of concrete..... 38
Figure 3.7 Tensile behaviour of steel reinforcement 39
Figure 3.8 Tensile behaviour of CFRP 41
Figure 3.9 Elements in FEM (ABAQUS Documentation, 2010) 42
Figure 3.10 Full vs reduced integration elements (ABAQUS Documentation, 2017) 42
Figure 3.11Solid element with different number of nods (ABAQUS Documentation, 2011)..... 43
Figure 3.12 Truss elements with different number of nods (ABAQUS Documentation, 2017)..... 44
Figure 3.13 Shell element with different number of nods (ABAQUS Documentation, 2017)..... 45
Figure 3.14 Bilinear traction separation law (Burlayenko & Sadowski, 2008) 48
Figure 3.15 Process of applying prestressing on the CFRP plate 50
Figure 3.16 Local coordinate system (ABAQUS Documentation, 2011)..... 50
Figure 3.17 Bonding at nodes between concrete and CFRP plate (ABAQUS Documentation, 2017)..... 51

Figure 3.18 Boundary condition and loading 52
Figure 3.19 Meshing of concrete beam 53
Figure 4.1 Dilation associated with sliding along microcracks and particles (Zhao & Cai, 2010) 55
Figure 4.2 Influence of various dilation angle 56
Figure 4.3 Influence of viscoplastic regularization 57
Figure 4.4 Influence of mesh refinement on yield load 58
Figure 4.5 Load deflection curve of controlled RC beam 59
Figure 4.6 Crack patterns of experimental test vs FE 60
Figure 4.7 Load deflection curve of RC beam strengthened with CFRP plate 62
Figure 4.8 Crack patterns of experimental test vs FE 62
Figure 4.9 Load deflection curve of RC beam strengthened with prestressed (5%) CFRP plate 65
Figure 4.10 Crack patterns of experimental test vs FE 65
Figure 4.11 Load deflection curve of RC beam strengthened with prestressed (20%) CFRP plate 67
Figure 4.12 Crack patterns of experimental test vs FE 67
Figure 4.13 Load deflection curve of RC beam strengthened with prestressed (30%) CFRP plate 69
Figure 4.14 Crack patterns of experimental test vs FE 70
Figure 5.1 Effect of prestressing levels of CFRP plate 77
Figure 5.2 Increasing in the flexural strength of retrofitted RC beam (%) vs steel grades (MPa) for yield loads with respect to the regular steel grade of 423 MPa 79
Figure 5.3 Increasing in the flexural strength of retrofitted RC beam (%) vs steel grades (MPa) for ultimate loads with respect to the regular steel grade of 423 MPa 80
Figure 5.4 Effect of different length of prestressed (5%) CFRP plate 82
Figure 5.5 Effect of Various width of 5% prestressed CFRP plate 86
Figure 5.6 Effect of various thickness of 5% prestressed CFRP plate 88

List of Tables

Table 3.1 Plastic damage parameters 31

Table 3.2 Materials properties of steel reinforcement 39

Table 3.3 Materials properties of CFRP plate 40

Table 4.1 Summary of experimental vs FE results for yield loads 71

Table 4.2 Summary of experimental vs FE results for ultimate loads 72

Table 4.3 Proposed parameters for modeling concrete 73

Table 4.4 Proposed parameters for modeling steel reinforcement 73

Table 4.5 Proposed parameters for modeling CFRP plate 74

Table 4.6 Proposed parameters for modeling the contact between CFRP plate and RC beam 74

Table 5.1 Effect of prestressing levels of CFRP plate 78

Table 5.2 Effect of steel grade on retrofitted rc beam with various prestressing's levels of CFRP plate 81

Table 5.3 Effect of different length of CFRP plate 83

Table 5.4 Effect of various width of CFRP plate 85

Table 5.5 Effect of various thickness of CFRP plate 87

Chapter 1: Introduction

1.1 General

Reinforced concrete (RC) is a widely used construction material due to its good strength, low cost, and constructability. RC can be used in various structures included buildings, bridges, and heavy structures. However, RC members experience deterioration caused by environmental attack, heavy traffic loads, and earthquakes. There are a number of rehabilitation techniques using different materials to overcome this degradation. One of theses techniques is applying high tensile strength fibre reinforced polymer (FRP) materials to the tensile face of the RC beam to enhance flexural performance.

FRP composites have become attractive retrofitting materials because of their low density, high tensile strength, resistance to corrosion, and ease of handling. FRP materials are applied to develop the flexural and shear performance of RC members. There are many types of FRP materials such as carbon fibre reinforced polymer (CFRP), glass fibre reinforced polymer (GFRP), and aramid fibre reinforced polymer (AFRP). Among other types of FRP materials, CFRP has the highest tensile strength, high modulus of elasticity, and excellent fatigue properties.

CFRP materials are available in different forms including plates, sheets, and circular rods. The plate has a large surface area that facilitates its attachment to the tensile surface of the RC beam by using bonding materials such as epoxy. Another attaching technique was introduced to reduce the environmental attack to CFRP plate and further enhance plate bond to concrete, which is near surface mounted (NSM). NSM techniques can be applied by cutting small grove into the RC beam.

Additionally, prestressing of CFRP plate in strengthening allows for the utilization of its high tensile strength, unlike sheet wrapping. Likewise, the prestressing of CFRP plate increases the flexural strength of concrete beams by reducing the internal stress on both the concrete and internal steel reinforcement.

Experimental testing is the most widely used method to determine the improvement of RC members strengthened with prestressed CFRP plate in the flexural response. However, experimental testing becomes a time consuming and costly process especially in investigating the effect of multiple parameters related to material properties, bonding techniques, and prestressing levels. Therefore, the finite element method (FEM) can be used to overcome such drawbacks associated with experimental testing by showing the trends of changing for various variables.

The nonlinear behaviour of complex and composite material such as concrete can be modelled using nonlinear FEMs. The proposed model on this study simulates the two main behaviours of concrete under the compression and tension, in addition to the internal steel reinforcement's behaviour. There are many commercial 3D FEM-packages to analysis complexes materials behaviour under many circumstances including ABAQUS, ANSYS, and ADINA (ABAQUS Manual, 2011) (ANSYS Manual, 2007) (ADINA Manual, 2002). However, they vary in capabilities of model the response of RC beam retrofitted by prestressing CFRP plate, which requires the nonlinear contact surface modelling, detailed mechanical properties of concrete and CFRP, and prestressing effect.

The main purpose of this research report is to investigate the structural behaviour of RC beams strengthened with prestressed CFRP plates and investigate the effect of different parameters on the structural performance of the strengthened beams. To verify the proposed models for RC beams strengthened with prestressed CFRP plates, the results of the FE analysis (FEA) were validated

with experimental data reported by Hajihashemi et al (2011). To develop an FE model that represents the RC beam retrofitted by prestressed CFRP plate, the following tasks should be considered:

- Modelling the RC beam as a composite of nonlinear concrete and elasto-plastic steel reinforcement, in addition to elastic materials that fails by maximum tensile strain for the CFRP composite material. Each of these materials exhibits different behaviour under loading.
- Modelling the interaction behaviour between the RC beam and CFRP plate, which plays a critical role in the strengthening performance because debonding at the concrete-CFRP interface is one of the most frequently reported failure modes.
- Modeling the prestressing effect of the CFRP plate and how the stresses are transferred to the RC beam.

1.2 Research Objective

The primary objective of this research is to develop an FE models that captures the behaviour of the RC beams strengthened with different prestressing levels of the CFRP plate. The specific objectives of this research are:

1. Develop an FE models to represent the flexural behaviour of the RC beams strengthened by prestressed CFRP plate.
2. Validate the FE models using experimental results.
3. Conduct a parametric study to investigate the effect of the prestressing level, steel strength and dimensions, including length, width, and depth, of CFRP plate.

1.3 Organization

This thesis is organized into six chapters:

- Chapter 2: Literature Review - In this chapter, an introduction to FRP materials and a summary of previous studies on the experimental and numerical modelling of the application of FRP in strengthening of RC structures is presented.
- Chapter 3: Development of Finite Element Model – this chapter includes a development of the details of the FEM including the materials models.
- Chapter 4: Results and Validation - This chapter presents the results of the FEM and compares the result with the experimental data in terms of load-deflection curves, failure modes, and cracks patterns. It is concluded with a discussion of the FEM findings.
- Chapter 5: Parametric Study - The effect of different parameters on the flexural response of RC beam strengthened by prestressed CFRP plate is investigated.
- Chapter 6: Conclusions and Recommendations.

Chapter 2: Literature Review

2.1 Introduction

The increase of service load applied to structures makes the strengthening of existing structures an economical necessity to meet safety and functional requirements. There are several techniques used for strengthening of RC structures using steel, and FRP materials (Hajihashemi et al., 2011; Nie et al., 2011) (Hajihashemi et al., 2011). For steel plate, strengthening by attaching steel plate would provide RC structure with more strength; however, it has some drawbacks such as steel heavy weight and its susceptibility to corrosion. On the other hand, FRP materials have many advantages such as light weigh, resistance to corrosion, and easily attached to RC members. This chapter presents a summary of the literature on the strengthening techniques for RC members in both experiments and nonlinear finite element analysis. The research needs in this area are highlighted.

2.2 Introduction to FRP

Fibre reinforced polymer (FRP) can be defined as a composite material that consists of fibres that are embedded in a polymer matrix, as shown in Figure 2.1 that are available in different forms such as plates, rods, and sheets. All these forms have been used in structural applications due to their high strength compared to conventional steel reinforcement. The characteristics of FRP materials depend on fibre and matrix types, and their volume fraction. They exhibit linear elastic behaviour until reaching failure stress as presented in Figure 2.2. There are some advantages of using FRP such as high strength, light weight, and corrosion resistance. Also, in flexural strengthening and new design applications, prestressing of FRP materials provides much higher

strength and delayed crack initiation of beams. There are various types of FRP materials that are used in civil engineering including carbon fibre reinforced polymers (CFRP), glass fibre reinforced polymer (GFRP), and aramid fibre reinforced polymer (AFRP). There are numerous codes, technical standards, and guidelines available to introduce design procedures and tests to determine the mechanical prosperities of FRP including ACI 440R, ISIS Canada, and ASTM D3039.

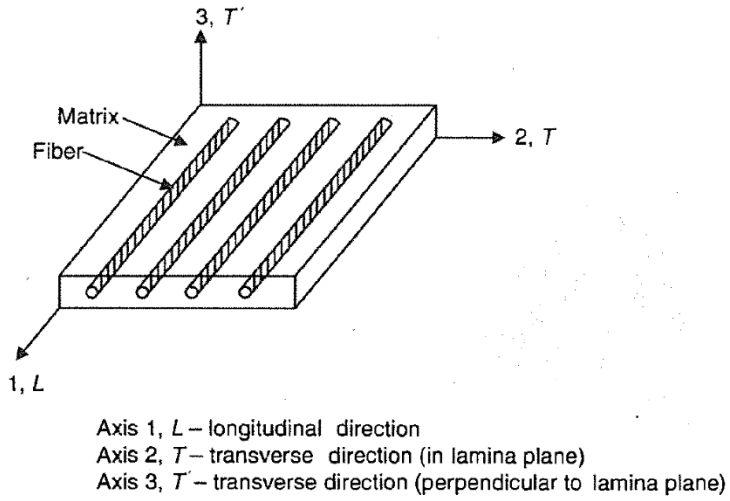

Figure 2.1Schematic representation of a unidirectional composite (Reddy, 2003)

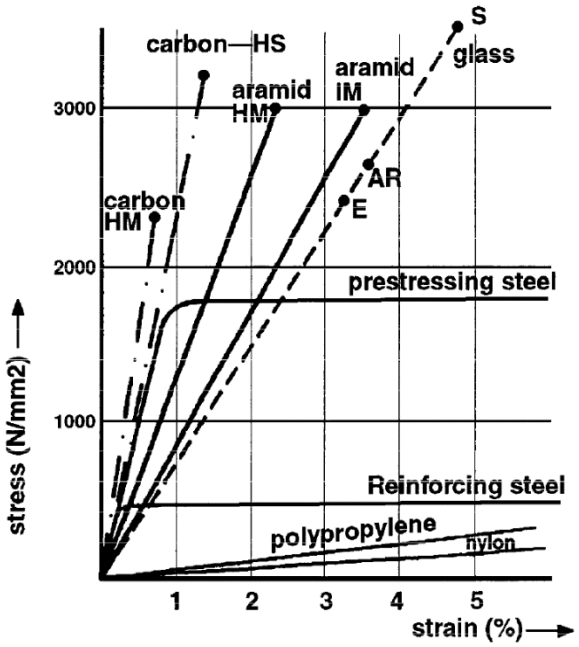

Figure 2.2 Tensile stress-strain behavior of various reinforcing fibres (ACI committee 440R, 1996)

2.2.1 Fibres

Continuum unidirectional fibres element acts as reinforcement in FRP composites due to their high axial strength and stiffness. The tensile strength of fibres mainly depends on the types of the fibres (carbon, glass, and aramid), volume fraction, and both the angle's orientation and alignments of the fibres. The fibres can be unidirectional or with different angle orientation, such as (0,45,90) shown in Figure 2.3. Also, there are other various alignment types for fibres in the laminate such as unidirectional, bidirectional, and pseudoisotropic as shown on Figure 2.4. Unidirectional fibres exhibit the highest strength and modulus on the fibre direction (Reddy, 2003) which makes it suitable for strengthening's applications. The angle's orientation of the fibre plays a major role in the laminate contribution to flexural and shear strength of the RC beam. To illustrate, if all fibres are unidirectionally aligned with an angle of 0^0 (i.e., fibres are parallel to longitudinal axis of the beam) which is used in flexural strengthening of RC beams. On the other

hand, if fibres are unidirectionally aligned with an angle of 90^0 (i.e., fibres are perpendicular to longitudinal axis of the beam) which is for the shear strengthening of RC members. In addition, the angle's orientation of the fibres plays critical role on the value of the interfacial stress between RC beams and CFRP plate (Krour et al., 2013). For instance, for fibres unidirectional aligned with angle of 90^0 the minimum value of shear and interfacial stress are obtained, while opposite obtained for fibres unidirectional aligned with angle of 0^0 (Krour et al., 2013). Moreover, the unidirectional FRP is considered orthotropic because the fibres filaments have higher strength and stiffness in the longitudinal direction than transverse directions. Different types of fibres have been used in manufacturing FRP composites including carbon, glass, and

aramid.

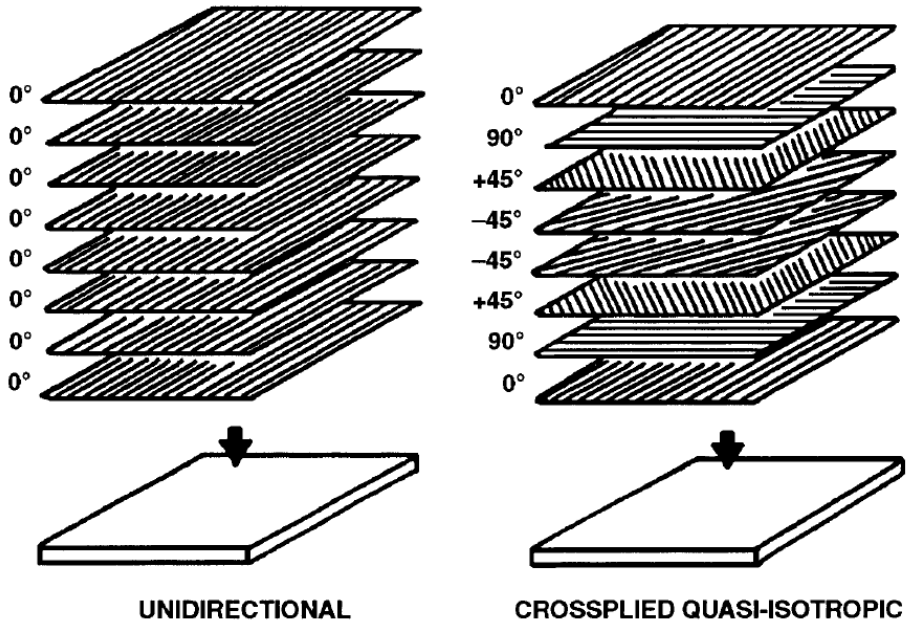

Figure 2.3 Varying fibre orientation (reproduced from ACI committee 440R, 1996)

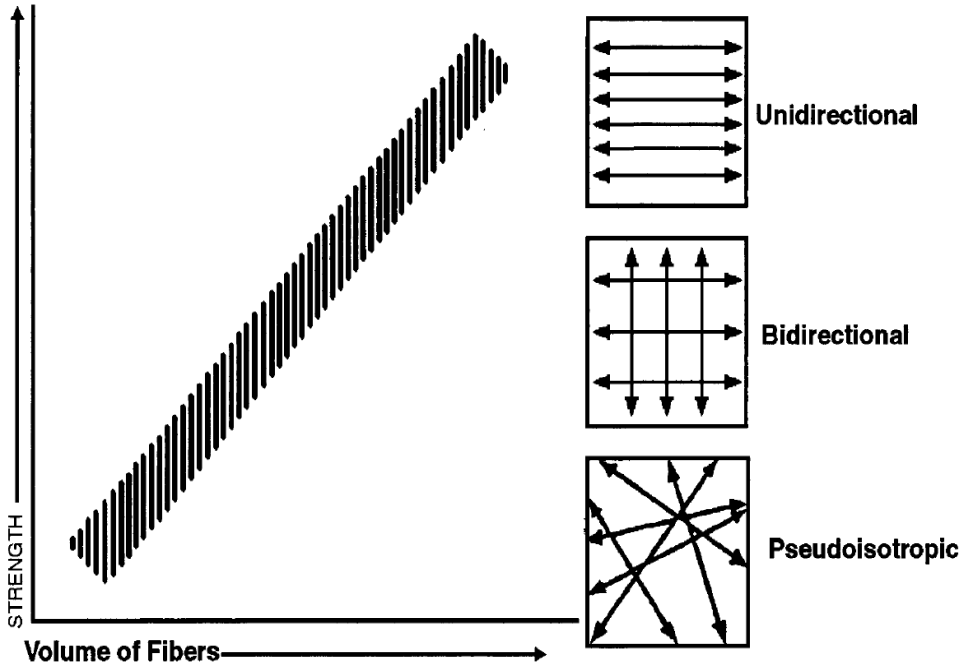

Figure 2.4 Strength relation to fibre orientation (reproduced from ACI committee 440R, 1996)

Carbon fibres have the best mechanical properties compared to other fibres due to their high tensile strength, good corrosion resistance, high strength to weight ratio, excellent fatigue resistance, low coefficient of thermal expansion, and high stiffness. However, high cost is a drawback for these fibres.

Glass fibres have some advantages of including low production cost, high tensile strength, outstanding heat resistance, and low electrical conductivity. However, glass fibres have lower stiffness and strength compared with carbon fibres.

Aramid fibres can be classified to be in the middle between carbon fibres and glass fibres because of their lower production cost than carbon fibres and higher stiffness than glass fibres. They have some advantages including high strength and good corrosion resistance.

2.2.2 Matrix

The matrix is a polymer resin that is usually made of vinylester or epoxy with some additives. The main role of matrix is to hold the fibres, protect fibres, and transfer the stress between fibres by the shear stress at the fibre-matrix interface. It is worth mentioned that the maximum strain of the matrix is higher than that of the fibres to avoid cracking the matrix before any cracks in the fibres. Figure 2.5 shows the schematic tensile stress-strain relationship for of FRP components.

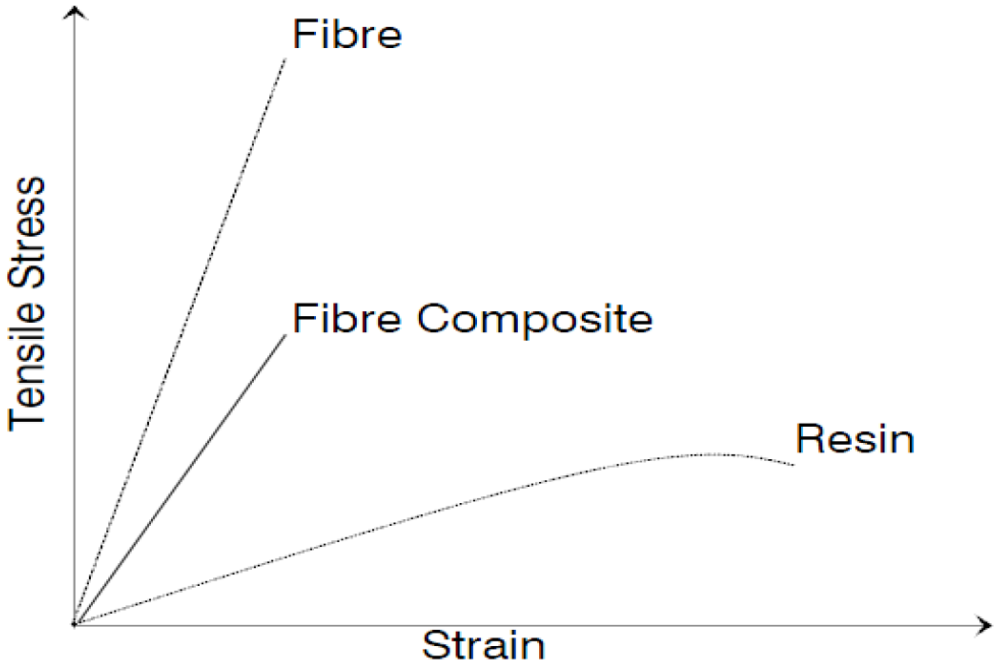

Figure 2.5 Tensile stress-strain relationships for the composite FRP and its components (reproduced from ACI committee 440R, 1996)

2.3 Bond between FRP Laminate and Concrete

Adhesive is used to attach the FRP laminate to concrete in the RC beams. The bond between concrete and FRP plays a critical role in transferring the load from concrete to FRP

laminate (Diab & Wu, 2007). Therefore, the properties of adhesive materials (bonding) must be well identified because their strength and stiffness have a direct impact on their adhesive function. The bonding between the FRP plates and RC members is classified as anisotropic due to the natural behaviour of FRP's materials. To illustrate, the nature of this anisotropic behaviour of FRP is due to the characteristics differences between the longitudinal behavior, which is dominated by the fibres, and the transverse behavior is controlled by the resin (Cosenza et al., 1997). There are many adhesive materials that can be applied between the RC concrete and CFRP laminate such as epoxies and viny ester. Losing the bonding materials is defined as bond failure; there are many failure modes that will be presented in section 3.5. Many research works have been conducted to investigate the delamination of FRP laminate from concrete members. They mainly focused on the bond strength and fracture energy. The relationship between the two is characterized using traction-separation model which often assumes linear elastic behaviour captured by the elastic tensor (K^0). Then, the damage mechanisms in traction separation starts when it reaches the damage initiation criteria (τ). After that, damage evolution law represents the damage evolution either by energy needed to open a crack (G_{cr}) or opening displacement at fracture (δ_{cr}). Figure 2.6 shows a bilinear traction separation law which combines both effective traction ($\boldsymbol{\tau}$) and opening displacement at fracture (δ_{cr}) (Burlayenko & Sadowski, 2008).

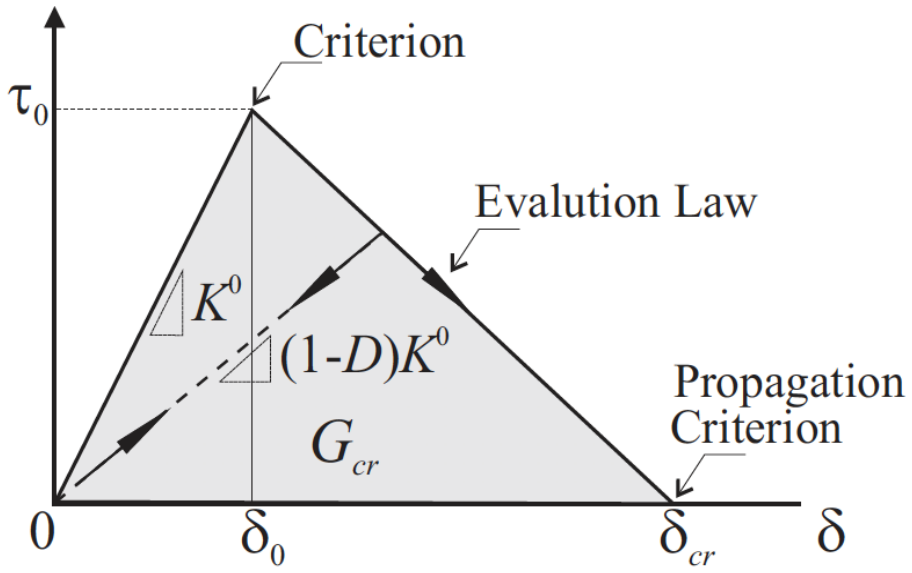

Figure 2.6 Bilinear traction separation law (Burlayenko & Sadowski, 2008)

2.4FRP as Strengthening Materials for RC Members

FRP composites have been commonly used as reinforcement and strengthening materials in civil engineering concrete structures in a from of internal or external reinforcement for the RC members. Internally, FRP composites are used instead of internal steel rebars. Externally, different forms of FRP laminate including sheets or plates are used in strengthening degraded structure. Applying FRP materials improve flexural response and shear capacity of RC members. To increase the flexural strength of reinforced concrete (RC), FRP sheets or plates are attached to concrete surface in the tensile zone using bonding materials such as epoxy which resulted in an increase in flexure strength by for example 10% (Hajihashemi et al., 2011) by releasing stress from the internal reinforcements. Moreover, increasing the shear capacity of RC members can be achieved by attaching the FRP laminate to the side of concrete beams at the zone of maximum shear resulting in higher ultimate strength of concrete beams (Abuodeh et al., 2020).

2.5 Advantages and Disadvantage of Using FRP for Strengthening RC Members

2.5.1 Advantages of using FRP

FRP composites have become popular materials that has been used to strengthen new or existing structures. There are some benefits of using such materials, as discussed below:

1) High tensile strength on the main axis of fibres (Reddy, 2003).
2) Light weight.
3) Durability.
4) The ability of prestressing (Hajihashemi et al., 2011).

2.5.2 Disadvantages of using FRP

Although there are many advantages of using FRP in strengthening of RC members there are some drawbacks that must be considered when using FRP with concrete. Firstly, some of these FRP materials are expensive such as carbon fibre reinforced polymers. Secondly, some of the FRP materials are very sensitive to some environment condition. For example, glass fibre is extremely sensitive to alkali attack in stressed environment. Finally, the lack of yielding is a common drawback as FRP materials behave elastically until failure stress.

2.6 Application of FRP in Civil Engineering

2.6.1 Introduction

FRPs have been used as strengthening and reinforcement materials in civil engineering structures (van den Einde et al., 2003). The role of FRP in civil engineering can be divided into two parts as shown in Figure 2.7 below (van den Einde et al., 2003). The first role is embedding FRP in new construction, this is mostly applied in the form of rods to utilize their benefits by design FRP/ concrete system (van den Einde et al., 2003). The second role is rehabilitating of

existing structures by attaching the FRP materials to existing structure using bonding materials (Hajihashemi et al., 2011).

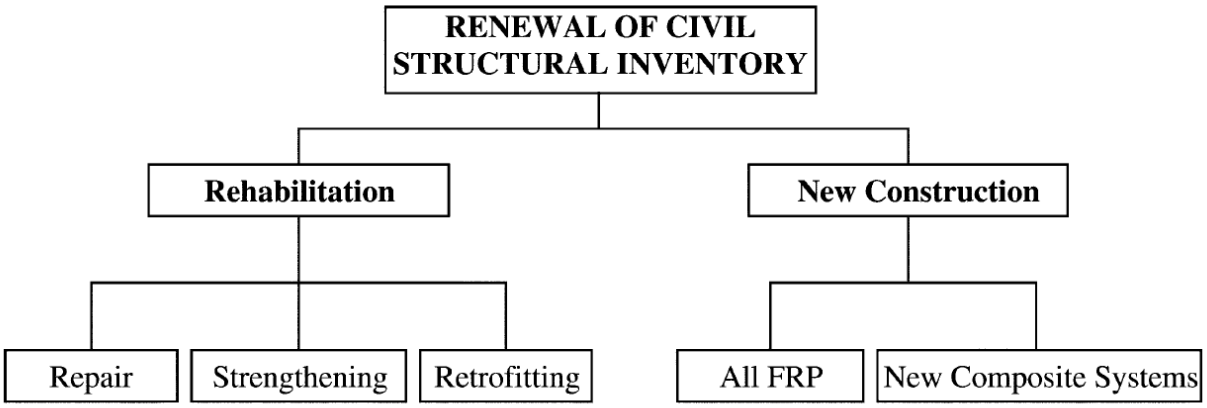

Figure 2.7Applications of FRP in civil engineering structures (van den Einde et al., 2003)

2.6.2 Methods of using FRP in RC Members

FRP has been used for retrofitting existing structures that are mostly degraded due to harsh environmental attach and subjected to increasing applied load. These applications of FRP are summarized as follows:

1) Near Surface Mounted Reinforcement (NSM): This application could be done by creating a groove near the surface of concrete. Furthermore, this technique has been introduced to perform site installation, and reduce debonding possibilities of the FRP plate because of easy anchorage options(Hajihashemi et al., 2011) (de Lorenzis & Teng, 2007).
2) Embedded Through Section (ETS): This method requires drilling vertical holes with specified spacing that must be created through the middle of the cross section of the RC beams. ETS technique improves bonding performance because of the greater confinement offered by the concrete core(Chaallal et al., 2011).

3) Prestressing of FRP: One of the most attractive benefits of using FRP is its the ability for prestressing which provides concrete with higher stiffness and delaying crack initiation (Hajihashemi et al., 2011).

2.6.3 Prestressing reinforcement on concrete

Many advantages can be gained by prestressing the reinforcement included increasing the yield load of RC members, reducing the stress in the internal steel reinforcement and reducing both size and spacing of the cracks. For example, prestressing CFRP plate between 40% and 60% were able to improve the yield load and ultimate load of RC beams by 60.1% and 59.8%, respectively compared to unstrengthened one as shown in Figure 2.8 (PFCU1: PFC refers to the RC beam with anchorage system, U1 refers to unbonded plate, and R refers to prestressing level 0 for non prestressed, 2 for prestressing with 20%, 4 for prestressing with 40%, and 6 for prestressing with 60%). Such advantages contribute to make prestressing an attractive method for strengthening the RC structure (Yang et al., 2009).

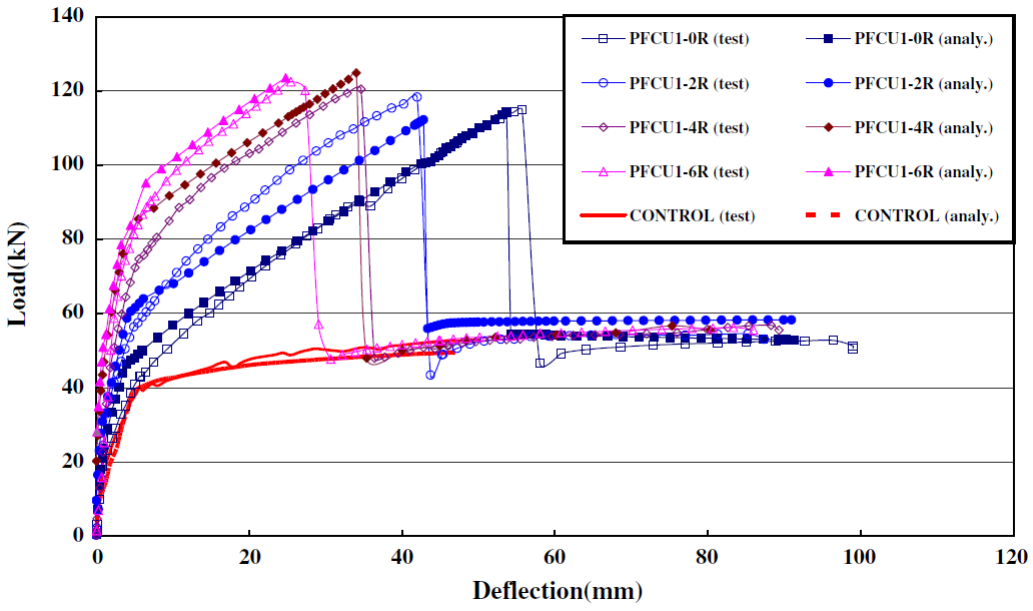

Figure 2.8 The effect of FRP prestressing level on RC beams performance (Yang et al., 2009)

There are two methods to apply prestressing that can be characterized based on the time of prestressing. First prestressing method is by adding the prestressing force before any contact of concrete with FRP or steel which defined as pretension. One of the prestressing's form is prestressing of external reinforcement such as FRP plate that attached on concrete element (Hajihashemi et al., 2011). The second form is prestressing of internal reinforcement where the same concept of the previous method applies but it is embedded reinforcement (Lou et al., 2016).

Posttensioning is considered the second method of prestressing. This type of stressing could be used with both the FRP and steel reinforcements after casting concrete and would improve the overall load carrying capacity (Ma et al., 2016) (Matta et al., 2009).

2.7 Failure Modes of RC Strengthened with FRP Laminate

The most desired mode of failure is the rupture of FRP laminate because it reflects the utilization of high load carrying capacity of FRP materials. Some analytical and experimental studies have been conducted to investigate the failure modes (Smith & Teng, 2002) (Garden & Hollaway, 1998) (Esfahani et al., 2007). There are mainly seven modes of failure reported in literature. First mode of failure is yielding of the steel reinforcement followed by rupturing of FRP laminate as shown in Figure 2.9(a). Second mode is the concrete failure in compression that can be associated with or without of yielding of steel reinforcement without any damage to the FRP laminate, as shown in Figure 2.9 (b). The third mode is caused by the inclined shear crack at the end of the laminate which is a brittle failure by debonding the FRP composites, as shown in Figure 2.9(c). Concrete cover separation is the fourth mode of failure where the interfacial shear and normal stresses at the end of plate increase resulting in cracking of concrete. Then, cracks propagate horizontally along the RC beam causing the concrete cover to separate with FRP

laminate, as shown in Figure 2.9 (d). The fifth mode of failure is the end interfacial debonding of FRP laminate. This is mainly caused by the high concentration of stress (shear stress) at the end of FRP laminate as shown in Figure 2.9 (e). The last two modes of failure are caused by high concentration of the normal stresses at the middle of concrete which produce and propagate the flexural cracks; however, the last mode of failure is caused by both shear and flexural crack as shown in Figure 2.9 (f) and (g), respectively.

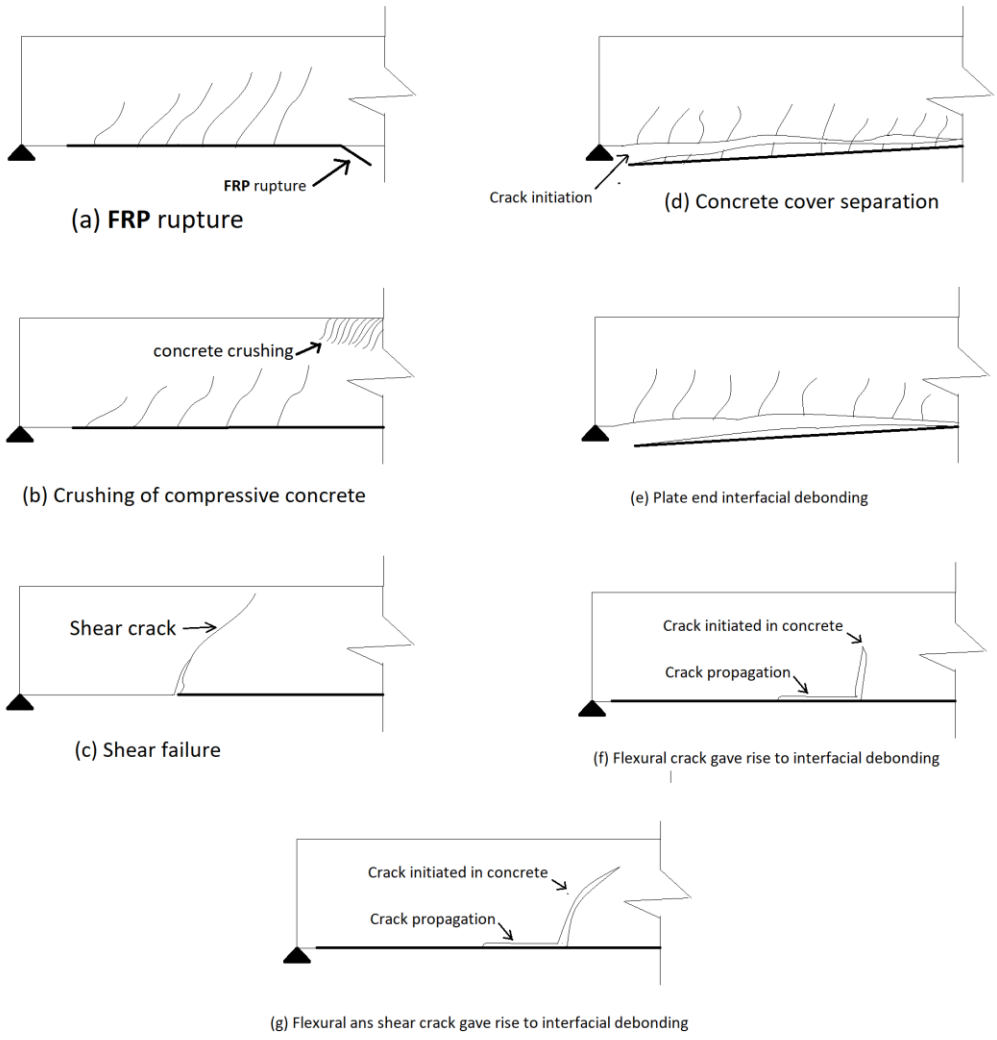

Figure 2.9 Failure modes of RC beams strengthened with FRP laminates

2.8 Experimental Research on Strengthening Concrete with FRP

Many experimental studies have been conducted on using FRP as strengthening materials in concrete structures. They covered the effectiveness of various applications of strengthening RC members with FRP reinforcement as presented below.

Toutanji and Gomez (1997) tested fifty-one RC beams under four-point bending to investigative the durability characterizations of interfacial bond between concrete and FRP sheet. Various variables were studied including different types of FRP sheets, harsh environmental conditions, and epoxy systems. It was concluded that using various types of FRP (carbon and glass) significantly improved the flexural performance in dry and normal conditions than in wet/dry condition. Debonding of the FRP sheet was the only failure mode and selecting of epoxy types played important role especially in wet/dry condition.

Yang et al. (2009) performed experimental study as well as 3D finite-element (FE) analysis using DIANA to investigate the flexure response of RC beams strengthened by prestressing CFRP plate. Four variables were investigated including bonding and no bonding of FRP plate, anchorage system, prestressing level (0% - 60%), and span length. It was concluded that the bonding had no effect on the performance of RC beams strengthened by prestressed CFRP plate. Also, RC beams strengthened with bonded CFRP plate without anchorage system shows lower ductility. The results of 3D finite-element (FE) showed a good agreement with experimental results.

An experimental study on fatigue performance of RC beams strengthened with prestressed CFRP plate was conducted by Peng et al (2016). Various strengthening techniques were applied including strengthening with and without prestressing of the CFRP plate. The results indicated that prestressed CFRP plate significantly improved the monotonic and fatigue performance of RC

beams. Also, prestressed CFRP plate profoundly reduced the deflection and stress in the steel reinforcement in the RC beams.

Badawi and Soudki (2009) performed both experimental and analytical studies on flexural behaviour of RC beams strengthened by prestressing near surface mounted (NSM) CFRP rods. Two levels of prestressing were applied: 40%, and 60% of ultimate tensile strength of the CFRP rod. It was concluded that prestressing of NSM CFRP rods were very effective technique that resulted in an increase of up to 90% in the yield load and up to 79% in the ultimate load compared to controlled beams.

Ye et al. (2002) investigated the shear strength of 7 RC columns strengthened by wrapping with CFRP sheets. Three variables were studied including CFRP sheets amount, shear span/depth ratio, and axial load ratio. It was reported that using CFRP sheets effectively improved the shear strength of RC columns after diagonal shear cracks occurred. However, using of CFRP sheets to improve the shear strength was only effective if the originally provided transfer reinforcement was not sufficient.

Brena et al. (2003) experimentally studied the effect of various strengthening configurations using CFRP sheets and plates on the flexural response of RC beams. A total of 20 RC beams were tested under four-point bending loading using various CFRP layouts. The first CFRP layout is attaching the CFRP plate to the bottom of the RC beams with and without CFRP sheets U-wraps anchorage. The second CFRP layout is attaching the CFRP sheets to the sides of cross section of RC beams without CFRP U-wraps. It was concluded that various configurations contributed to make RC beams stiffer compared to control beam and strengthening with CFRP sheets U-wraps delayed or prevented of debonding of CFRP plates.

El-Hacha and Rizkalla (2004) studied the flexural improvement of RC beam using near surface mounted (NSM) FRP plates and rods. Various variables were investigated including different FRP systems (rods and plates), using GFRP and CFRP materials. Both of NSM FRP carbon and glass exhibited the same axial stiffness. The results showed that strengthening the RC beams with NSM CFRP plates exhibited higher load carrying capacity than NSM CFRP rods because of early debonding between CFRP rods and epoxy.

Chaallalet al. (2011) performed experimental investigation on the effectiveness of embedded through section (ETS) technique for enhancing the shear capacity of RC T-beams by using FRP rods. They examined various FRP techniques including externally bonded (EB) FRP sheets, near surface mounted (NSM) FRP rods, and ETS FRP rods, in addition to the presence of transfer reinforcements. They reported that using ETS technique for shear strengthening of RC T-beams with FRP rods had the highest improvement of shear capacity with 60% compared to 23%, and 31% for EB FRP sheets, and NSM FRP rods, respectively. Also, ETS FRP strengthening improved the shear capacity of RC beams with presence of transfer reinforcement, while EB FRP sheets and NSM FRP rods had less impact on the shear capacity of RC members with presence of transfer reinforcement. Such conclusion was attributed to the confinement effect of concrete core because of embedding the FRP rods.

Al-Tamimi et al. (2011) studied experimentally the effect of repairing of self consolidating concrete (SCC) RC beams with various ratios of CFRP plate length to shear span and anchorage on the flexural behaviour. Various ratio of CFRP plate length to shear span included 0.25.70, and 85% that were used with and without end anchored for one or two CFRP layers of U-wrap sheets under monotonic loading. It was found that there is an increase of 5 to 80% in the load carrying capacity of strengthened RC beams compared to control RC beams. It was also reported that

strengthening with 25% as ratio of CFRP plate length to shear span length of RC beams with appropriate end anchorages was sufficient to strength the RC beams.

Dias and Barros (2013) conducted a study on the shear strengthening of RC beams using NSM CFRP plates and analytical modeling. They examined various variables including concrete strength, percentage of steel stirrups, inclination of CFRP plates, and existence of cracks. They concluded that increasing effectiveness of NSM CFRP plates was related to the increase of concrete strength, and the efficiency of strengthening using NSM CFRP plates was obvious with lower steel stirrups ratio. It was also reported that using inclined CFRP plates provided RC beams with more shear resistance than vertical CFRP plates, as well as there was a delay on presenting cracks when the RC beams strengthened with CFRP plates.

Both experimental investigation and 3D finite-element (FE) development for new NSM CFRP reinforcement techniques' effect on flexural capacity of RC members were conducted by Rezazadeh et al. (2016). New configuration of CFRP was introduced which combined both NSM and external bonded reinforcement (EBR) by manufacturing T-shaped CFRP profiles. They concluded in their experimental results, that using new system of reinforcement for flexural strengthening with varying T-shaped CFRP profiles had improved the load carrying capacity between 114.6% and 252.01%; however, there was a reduction in the strain profiles in CFRP reinforcement. A good agreement between FE results and experimental results was reported. Three parametric studies were performed including varying modulus of elasticity of CFRP, strength of concrete and concrete-epoxy interface, and ratio of CFRP profiles. It was reported that increasing the modulus of elasticity of CFRP would increase both flexural stiffening and load carrying capacity of RC members however at the expense of reduction of ultimate deflection capacity. It was also mentioned that reducing both strength of concrete and concrete epoxy interface would

reduce the ultimate load carrying capacity and deflection capacity. The final conclusion was using larger bond area and cross-sectional area of CFRP would enhance the load carrying capacity. Such conclusion was explained as using higher ration of CFRP provided higher resistance to tensile concrete cover splitting failure due to higher confinement of surrounding concrete to CFRP profile.

2.9 Numerical Research on Strengthening Concrete with FRP

A number of numerical investigations have been conducted on the applications of FRP as strengthening materials for RC members. Different FE packages were used to simulate the experimental response of different FRP techniques on RC members. Many models have been integrated in these simulations such as various materials, and cohesive interface models. Some of the numerical investigations are presented here.

Nonlinear finite element analysis to estimate the response of RC beams strengthened with FRP plates without prestressing on both the bottom or both sides of beams were performed by Hu et al (2004) using ABAQUS finite element package (Dassault Systems, 2018). All the results were compared with experimental data with a good agreement. Parametric studies were performed to investigate the effect of fibre orientation, beam length, and reinforcement ratio on the ultimate strength of concrete. It was found that the influence of beam's length on the flexural behaviour of RC beam strengthen with FRP plates on the bottom of the beam with low internal reinforcement ratio was higher than those with high internal reinforcement ratio. Also, more cracks were observed on the central area in the case of RC beam strengthened with FRP plates on the bottom with high internal reinforcement ratio compared to those with lower internal reinforcement ratio. However, the occurrence of cracks closed to supports were only limited to the case of FRP plates on the bottom with lower internal reinforcement ratio. Moreover, the effect of RC beams strengthened by different fibres orientation FRP on both sides were varied between long and short

length of the beam. For long beam, when the number of FRP layers was small, the ultimate load was less influenced by the angle of fibres ∅. For short beam, the zero degree was the ideal fibre angle with different conditions varied reinforcement ratio and numbers of FRP layers. The final observation in this paper was that increasing the bending resistance is more crucial than developing the shear resistance of the beam. Such conclusion was explained as using FRP plates at the bottom of RC beams provided higher ultimate load than those with $[\pm\ \emptyset]_n$ FRP plates on both sides.

Ebead and Marzouk (2005) investigated the ability of modeling flexural behaviour of FRP plates that strengthening RC concrete two-way slabs by using tension stiffening model integrated with ABAQUS. The bond between the FRP plates and concrete was modeled to be perfect since the FRP plates were embedded in the concrete slab. It was concluded that using the proposed tension stiffening and perfect bond model between FRP plates and concrete slab were adequate to represent the real response for the experimental conditions.

Obaidat et al. (2010) simulated the effect of CFRP plate and CFRP plate/ concrete interface models for RC beams using ABAQUS; the results were compared with experimental one. Two types of models were used to model CFRP plate linear elastic isotropic and orthotropic. It was found that both models could represent the CFRP behaviour. Two types of interaction bond included perfect bond and cohesive bond models were evaluated to represent an accurate response of CFRP plate/concrete interface response. They concluded that cohesive bond model was able to accurately represent the real behaviour while perfect bond failed to represent the real behaviour.

Coronado and Lopez (2010) developed 3D finite-element (FE) to predict the response of RC beams strengthened with both FRP sheets and plates using ABAQUS. Debonding failure of the interface between the concrete and epoxy was modeled by using damage band (crack band),

and the results were compared with the experimental findings. The results confirmed that using crack band was proper to simulate the debonding between concrete and FRP sheet and plates.

Hawileh et al. (2011) numerically investigated the flexural response of cantilever RC T-beam strengthened in shear with side bonded CFRP sheet under cyclic loading using ANSYS finite element package. To model the bonding between the CFRP sheets and concrete, a shell element was used as a thin layer with materials properties was used and was represented the real behaviour observed experimentally. Different parameters were investigated including various spacing of CFRP sheet, number of CFRP sheet layers, and fibre orientations. It was reported that increasing spacing between CFRP strips contributed to create larger crack propagation. It was also noticed that using 2 and 3 layers of CFRP sheets increased the failure load by 5.31% and 14.38%. It was concluded that strengthening by external CFRP sheets provided RC T-beam with maximum load at failure, whereas strengthening by using inclined CFRP sheets orientations ($+45^o$ and -45^o) provided RC beams with highest deflection at failure.

Another similar numerical study conduced by Hawileh et al. (2013) to investigate the performance of RC beams strengthened with CFRP plates which covers 25% of shear span and CFRP plates bonded to the soffit of the beam with and without anchoring of different arrangement of CFRP U-wrap sheets. Bond slip model was used to model the contact between steel rebars and concrete, and interface cohesive model was applied to simulate the concrete-CFRP plate interface. Different parameters were investigated namely: different diameters of tensile steel reinforcements and both the width and arrangement of CFRP U-wrap sheets. It was reported that increasing the cross-sectional area of tensile steel reinforcements would decrease the beam's ductility. The authors also indicated that the ideal configuration of CFRP U-wrap sheets was by using two sheets that perpendicular to each other with width of 400 mm.

Hawileh (2012) numerically examined RC beams strengthened with NSM FRP rods by using ANSYS. Bond slip model and interface cohesive model were used to model the contact between steel rebars and concrete, and concrete-CFRP rods interface, respectively. Various parametric studies were investigated including materials type and diameters of FRP rods. It was stated that strengthening by CFRP rods provided RC beams with higher ultimate strength by 18.5% and 43.8% than those RC beams strengthened with AFRP and GFRP rods, respectively. It was also found that increasing the diameter of FRP reinforcement noticeably increased the failure load.

Godat et al. (2013) incorporated 2D and 3D FE to estimate the interface properties of embedded through section (ETS) FRP/ concrete and load deflection relationships of RC T-beam strengthened for shear with FRP rods. All the FE models were developed by using ADINA finite element package, and the perfect bond was assumed for the case of ETS FRP rods. 2D FE was developed to simulate pullout results for ETS FRP and concrete. The numerical results were almost the same results as the experimental one. It was also found that 3D FE models using perfect bond model between RC members and ETS FRP rods were able to accurately represent the experimental behaviours of RC T-beam strengthened in shear with ETS FRP rods. Such results were explained as the failure mode in the experiments was not the debonding mode.

de Domennico et al. (2014) devolved a new FE-based methodology to anticipate the peak load and failure mechanism of failure of RC members strengthened with internal FRP rods by using ADINA. The results of six RC beams and six RC slabs strengthened with internal FRP rods under four-point bending were used to validate the results. Modified nonstandard constitutive flow law for concrete which combines both kinematic and static approach of limit analysis to provide upper and lower peak load values respectively was introduced. Moreover, the proposed model was

used to represent the experimental behaviours of RC members. It was verified that proposed models were able to accurately exhibit the real behaviour observed in the experiments.

2.10 Conclusion

FRP strengthening techniques has been used to retrofit deficient RC members. Many experimental investigations have been conducted on the effectiveness of using FRP techniques including various applications such as flexural and shear strengthening, configurations, number of layers, orientations, and prestressing levels. All the previous studies confirm that FRP is such an attractive method for providing RC members with strength. Several numerical packages were used to simulate most of the experimental tests which showed a good agreement with results of tested studies. To the author's knowledge, there were not enough studies reported on the use of FE packages to simulate the effect of prestressing level on the FRP sheets or plates. Consequently, this research aims to fill this gap to support the research field with an efficient analytical model that can save time, cost, and consequently natural resources.

Chapter 3: Development of Finite Element Model

3.1 Introduction

Finite element (FE) modeling has been used extensively due to its efficiency and reasonable accuracy in analyzing structural behaviour of concrete under different loading conditions. Although experiment tests are the most reliable, there are a number of drawbacks associated with these tests such as the difficulty of applying some loading and boundary conditions, long preparation and testing time, and high cost. ABAQUS FE package was used for its capability to simulate different concrete, steel, and CFRP components, in addition to model the assembly of these components using advanced interfacial models between concrete and CFRP plate.

This chapter presents the development processes of models. This includes beam geometry, materials' properties of each part, boundary condition, elements selection, meshing, contact modeling between components, and applying prestressed force.

A full section was dedicated to materials' properties. Concrete material properties was presented in details as it exhibited complicated non-linear behaviour that varied between tension and compression stresses. Also, the contact between CFRP plate and concrete, some interfacial parameters are required to accurately represent the delamination process at the contacting nodes.

3.2 Model Configuration

The parameters that were used for experimental tests by Hajihashemi at al. (2011) were used as input parametrs in these models to have comparable results. The dimensions of expermental beam were $3300 \times 350 \times 300$ mm with a groove of 25×5 mm on the concrete surface as shown in Figure 3.1. The total span between two supports was 3000 mm. For tensile steel reinforcement, each beam was reinforced with five steel rebars with a diamaterter of 20 mm. For compressive steel reinforcement, each beam was reinforced with two steel rebars with a diamaterter of 14 mm. For shear reinforcement, stirrups of ($\emptyset 10$) mm were used at 75 mm intervals along the beam. The CFRP plate has a rectangular section of 25 mm widht and 2 mm thickness applied along the full length of external tenstion face of the beam.

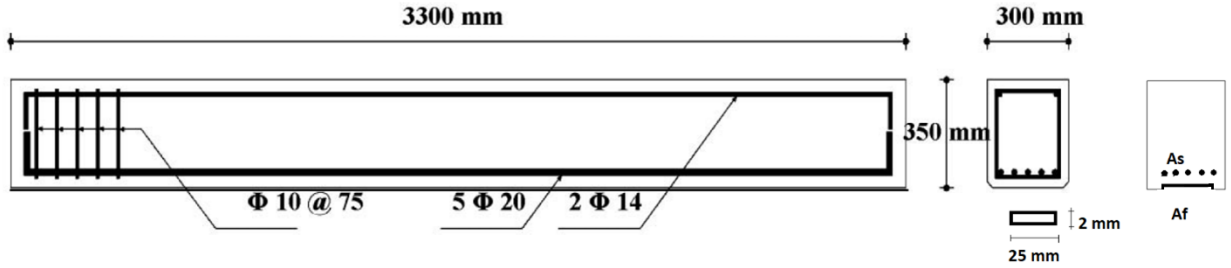

Figure 3.1 Dimensions of experimental beam with CFRP plate (Hajihashemi, et al., 2011)

Due to the symmetry of the RC beam and CFRP plate, applying load, materials properties, and boundary conditions, only half of the beam was modeled to reduce the computation time. The concrete beam was created using 3D deformable solid part as shown in Figure 3.2. For the steel reinforcement, a deformable wire part with truss element was used to build that part due to its ability to represent steel reinforcement and reduce computation time as shown in Figure 3.2. Moreover, stirrups for the shear reinforcement were created by deformable wire part with truss

elements as shown in Figure 3.2. Finally, the CFRP plate was modeled using shell elements as shown in Figure 3.2.

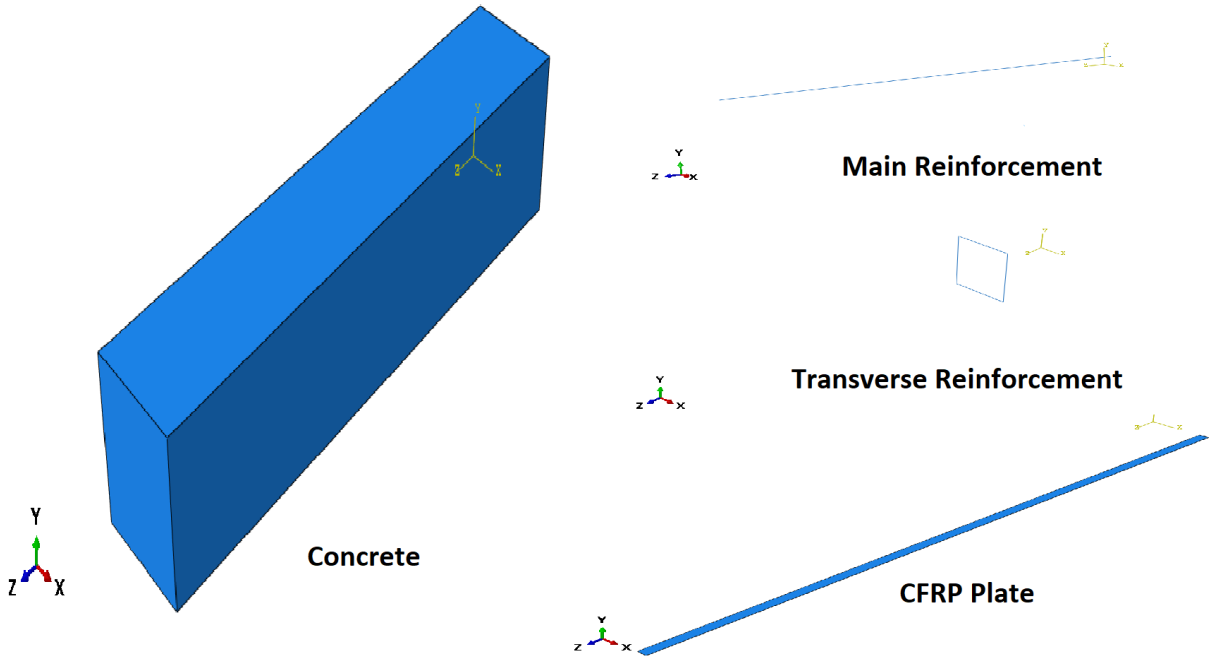

Figure 3.2 Parts of the FE model of the beam, steel reinforcement and stirrups and CFRP plate in ABAQUS

3.3 Materials Modelling

Well-defined materials properties are essential for accurate FE modeling. In FEM, there is a wide range of materials properties that aim to simulate the real behaviour of each part. Some of these behaviors need a specific model such as the Concrete Damage Plasticity (CDP) available in ABAQUS. In this study, three main materials are modeled, namely: concrete, steel, and CFRP. Each of these materials will be discussed in detail on next sub-sections.

3.3.1 Concrete

Concrete is a composite material made of cement, coarse aggregate, fine aggregate, and water. Due to the nature of different materials that make up the concrete mix, concrete exhibits

non-linear stress strain relationship. Also, concrete has different behaviour under tension and compression as it is clearly demonstrated by its higher compression strength compared with tensile strength. This is attributed to the interaction between cement and both types of aggregate, in addition to different components behaviour under loading. Various approaches have been used to model concrete behaviour under different loading conditions. These include smeared crack model (SCM), brittle cracking model (BCM), and concrete damage plasticity model (CDP). The SCM model is applied to represent discontinues brittle behaviour of cracked concrete by only tracking the tensile failure for every integration point. The BCM model is used to model materials behaviour that is controlled by tensile cracking such as ceramics. On the other hand, the CDP captures two main failures of concrete which are compressive crushing and tensile cracking. After carefully reviewing the three above-mentioned models, it was found that the CDP is highly adaptable to model concrete behaviour under diverse loading conditions. Thus, the CDP was used to simulate the behaviour of reinforced concrete in this thesis.

3.3.1.1 Concrete Damaged Plasticity (CDP) Model

This model considers two main failure modes of concrete which are crushing stress under compression and cracking stress under tension. Elastic modulus, and Poisson's ratio are used to represent the elastic behaviour. On other hand, five plastic damage parameters are used to model the plastic part. They are the dilation angle (ψ), flow potential ratio, eccentricity, the ratio of initial equi-biaxial compressive yield stress (f_{b0}) to initial uniaxial compressive yield stress (f_{c0}), the ratio of the second stress invariant on the tensile meridian to that of compressive meridian (K), and the viscosity parameter that defines visco-plastic regularization (ABAQUS Documentation 2011). These parameters are provided in Table 3.1.

Table 3.1Plastic damage parameters

Parameter	Value
Dilation Angle (ψ)	30
Eccentricity (ϵ)	0.1
f_{b0}/f_{co}	1.16
K	0.667
Viscosity Parameter (μ)	0.001

Compression Model

Uniaxial compressive behaviour of concrete in the CDP model follows the general stress-strain curve as shown in Figure 3.3. The stress- strain behaviour can be divided into three stages:

1) Linear behaviour within the elastic region until the initial yield stress.
2) Plastic behaviour after reaching initial yield stress and shows strain-hardening behaviour until reaching ultimate stress.
3) Strain softening after reaching the ultimate stress.

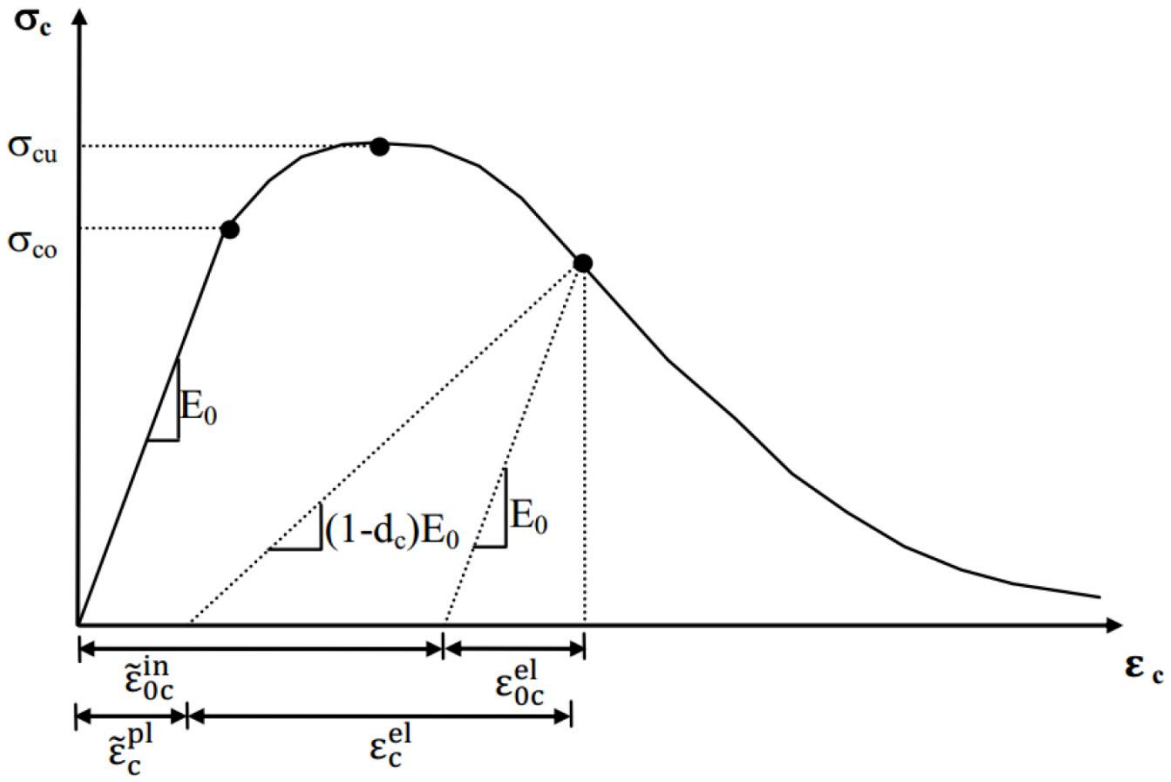

Figure 3.3 Compressive stress-strain relationship (ABAQUS Manual, 2011)

To model elastic stage, modulus of elasticity (E_o), and Poisson's ratio are required. The Poisson's ratio of concrete is varied from the value of 0.15 to 0.22. In this study, the value of Poisson's ratio for concrete is 0.2. Additionally, to model the behaviour beyond elastic region, compressive stress and inelastic strain values at multiple intervals (in tabular format) are required.

The stress-strain behaviour of concrete in compression can be obtained by experimental results, or by numerical technique proposed and validated by (Mitchell & Collins, 1978). In this thesis, the empirical technique is used instead of experimental results. The inelastic strain is expressed in equation 3.1:

$$\varepsilon_c^{in} = \varepsilon_c - \varepsilon_{oc}^{el} = \varepsilon_c - \frac{\sigma_c}{E_o} \qquad (3.1)$$

$$\varepsilon_c^{pl} = \varepsilon_c^{in} - \frac{d_c}{(1-d_c)}\frac{\sigma_c}{E_o} \quad (3.2)$$

Where:

ε_c^{in}: the inelastic strain.

ε_c^{pl}: the plastic strain.

ε_c : the total compressive strain.

ε_{oc}^{el} : the elastic compressive strain corresponding to undamaged materials.

σ_c : the compressive stress

E_o : the initial undamaged modulus of elasticity.

d_c : the concrete damage in compression.

The 28 days compressive strength of concrete (f_c') used in this study after 28 days was 31 MPa (Hajihashemi, et al., 2011). The numerical method validated by (Collins & Mitchell, 1978) was used in this work to model the behaviour of concrete as it is only limited to the case where the strength of concrete is lower than 41 MPa. The compressive stress strain curve was created by equations that are used for Hognestad parabola as shown below:

$$\sigma_c^1 = E_c\,\varepsilon \qquad \text{Where} \quad \sigma_c^1 < 0.4\acute{f}_c \quad (3.3)$$

$$\sigma_c^2 = \acute{f}_c\left(\frac{2\varepsilon}{\varepsilon_0} - \left(\frac{\varepsilon}{\varepsilon_0}\right)^2\right) \qquad \text{Where} \quad \sigma_c^2 > 0.4\acute{f}_c \quad (3.4)$$

$$\varepsilon_0 = \frac{2\acute{f}_c}{E_c} \quad (3.5)$$

$$E_0 = 4500\sqrt{f_c'} \tag{3.6}$$

Where:

σ_c^1: Concrete compressive stress which is the end of the elastic zone.

σ_c^2: Concrete stress until the after the elastic zone and corresponding to a given concrete strain.

ε: Concrete compressive strain which is the end of the elastic zone.

ε_0: Concrete strain corresponding to a given concrete stress (σ_c^2).

E_0: Young's modulus of concrete.

Using the previous equations, the Hognestad parabola was created to provide ABAQUS with stress strain curve that represents the compressive behaviour under compression as shown in Figure 3.4.

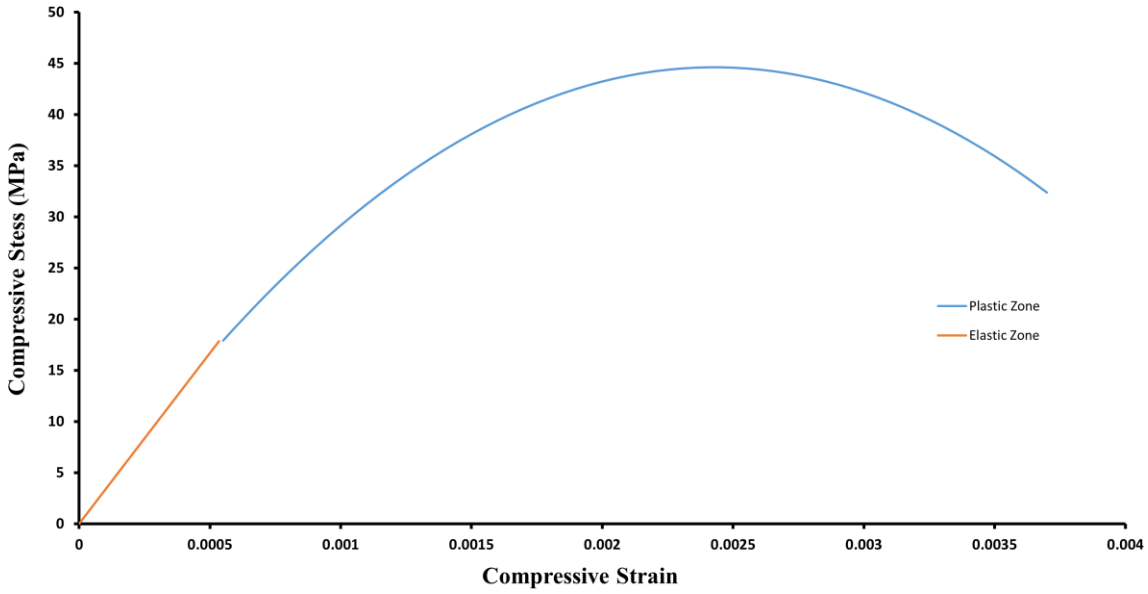

Figure 3.4 Compressive behaviour of concrete

Tension Model

Uniaxial tension behaviour of concrete in CDP follows the general stress-strain curve shown in Figure 3.5. The stress-strain relation is linear until the tensile strength (σ_{t0}) is reached, at which the cracking occurs. Then, concrete exhibits strain softening. In order to model the elastic zone, modulus of elasticity ($E_{o,}$) and Poisson's ratio are required. Additionally, to model the behaviour after elastic region, the tensile stress (σ_t) and inelastic strain (ε_c^{in}) in tabular format are needed. The inelastic strain is expressed in equation 3.2:

$$\varepsilon_t^{in} = \varepsilon_t - \varepsilon_{ot}^{el} = \varepsilon_t - \frac{\sigma_t}{E_o} \tag{3.7}$$

$$\varepsilon_t^{pl} = \varepsilon_t^{in} - \frac{d_t}{(1-d_t)}\frac{\sigma_t}{E_o} \tag{3.8}$$

Where:

ε_t^{in}: the inelastic strain.

ε_c^{pl}: the plastic strain.

ε_t : the total tensile strain.

ε_{ot}^{el} : the elastic tensile strain corresponding to undamaged materials.

σ_t : the tensile stress

E_o : Young's modulus of concrete.

d_t : the concrete damage in tension.

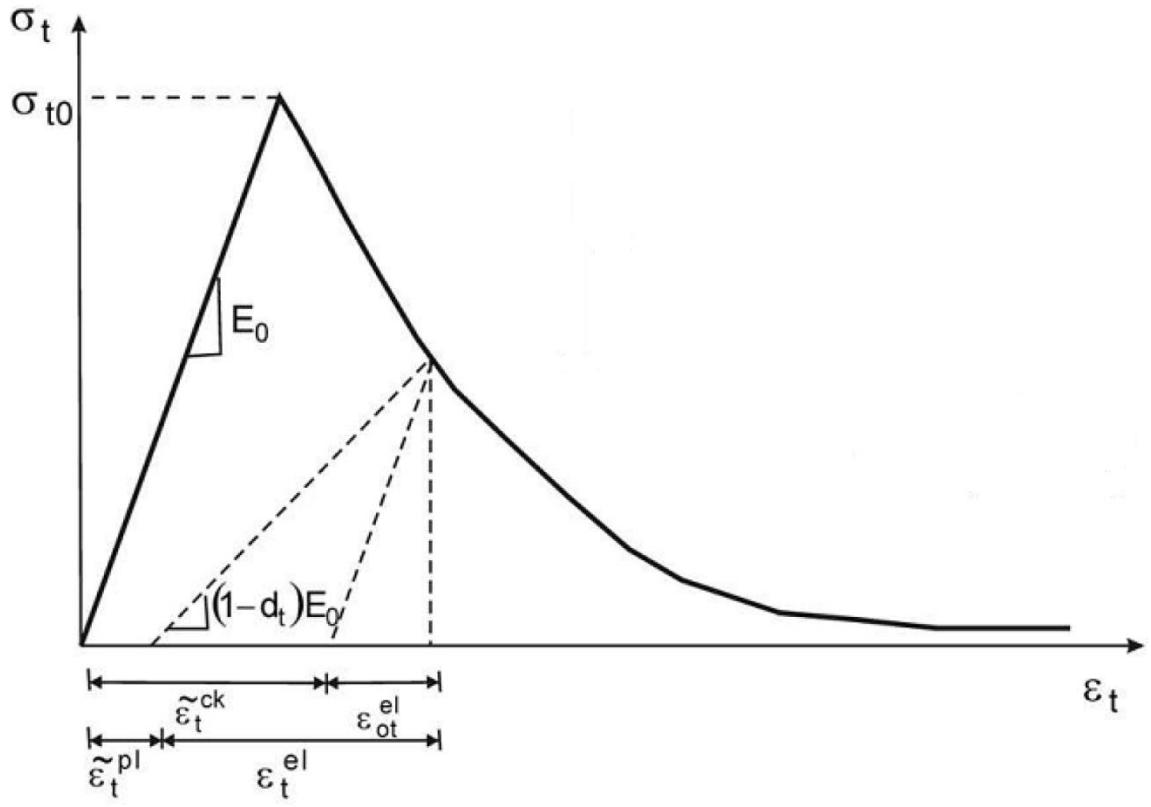

Figure 3.5 Tensile stress-strain relationship (ABAQUS Manual, 2011)

After cracking, the concrete can carry the tensile loading. The contribution of concrete in carrying loads after cracking is defined as "tension stiffening". This ability of concrete can be defined by providing the post peak response of concrete under tensile loading. There are three methods in ABAQUS to simulate this tension stiffening by defining the tensile stress of concrete as a function of cracking strain, displacement, and fracture energy. In this model, tension stiffening of concrete is defined by using cracking method due to its time efficiency to analyze the model, as shown in Figure 3.6. In this method, Tensile stress must be provided as function of cracking strain as shown in equations below:

$$\sigma_t^1 = E_o \varepsilon_t \qquad \text{Where } \varepsilon_t < \varepsilon_{cr} \tag{3.9}$$

$$\sigma_t^2 = f_t^{'} \left(\frac{\varepsilon_{cr}}{\varepsilon_t}\right)^{0.4} \text{ Where } \varepsilon_t > \varepsilon_{cr} \tag{3.10}$$

$$\varepsilon_{cr} = \frac{f_c^{'}}{E_o} \tag{3.11}$$

$$E_o = 4500\sqrt{f_c^{'}} \tag{3.12}$$

$$f_t = .33\sqrt{f_c^{'}} \tag{3.13}$$

Where:

σ_t^1: Concrete tensile stress which is the end of the elastic zone.

σ_t^2: Concrete stress after the elastic zone and corresponding to a given concrete strain.

ε_{cr}: Concrete tensile strain which is the end of the elastic zone.

ε_t: Concrete strain corresponding to a given concrete stress (σ_t^2).

E_{co}: Young's modulus of concrete.

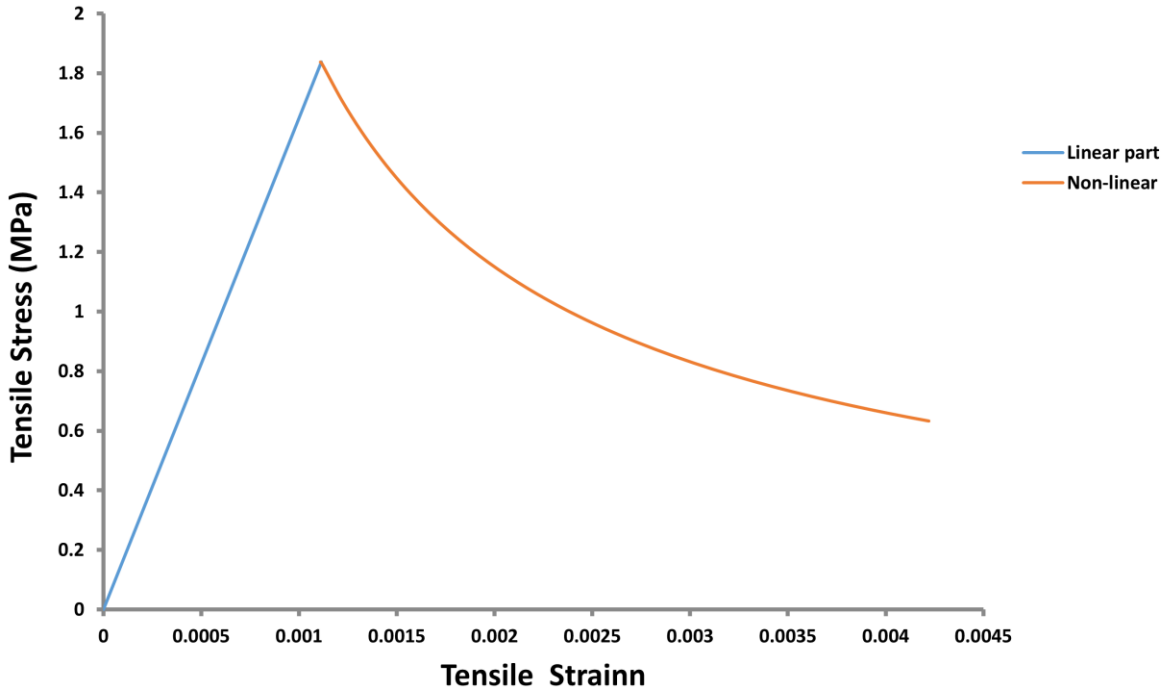

Figure 3.6 Tensile behaviour of concrete

3.3.2 Steel

Steel reinforcement bars with a yield stress of 423 MPa were used in this thesis. For tensile steel reinforcement, five steel rebars were used with a diamaterter of 20 mm. For compressive steel reinforcement, two steel rebars with a diamaterter of 14 mm. For shear reinforcement, stirrups of (Ø10) mm were used at intervals 75 mm along the beam. The materials proprieties of steel reinforcement are provided in Table 3.2. In this model, the reinforcement element is elastic perfectly plastic as shown in Figure 3.7 without considering the steel hardeing since it shows no differences when it was applied . The equation for stress strain curve is presented:

$$f_s = \varepsilon_s E_s \tag{3.14}$$

Table 3.2 Materials properties of steel reinforcement

Materials Property	Value
Modulus of Elasticity ($\boldsymbol{E_s}$)	200 GPa
Poisson's Ration ($\boldsymbol{\nu}$)	0.3
Yield Stress ($\boldsymbol{f'_s}$)	423 MPa

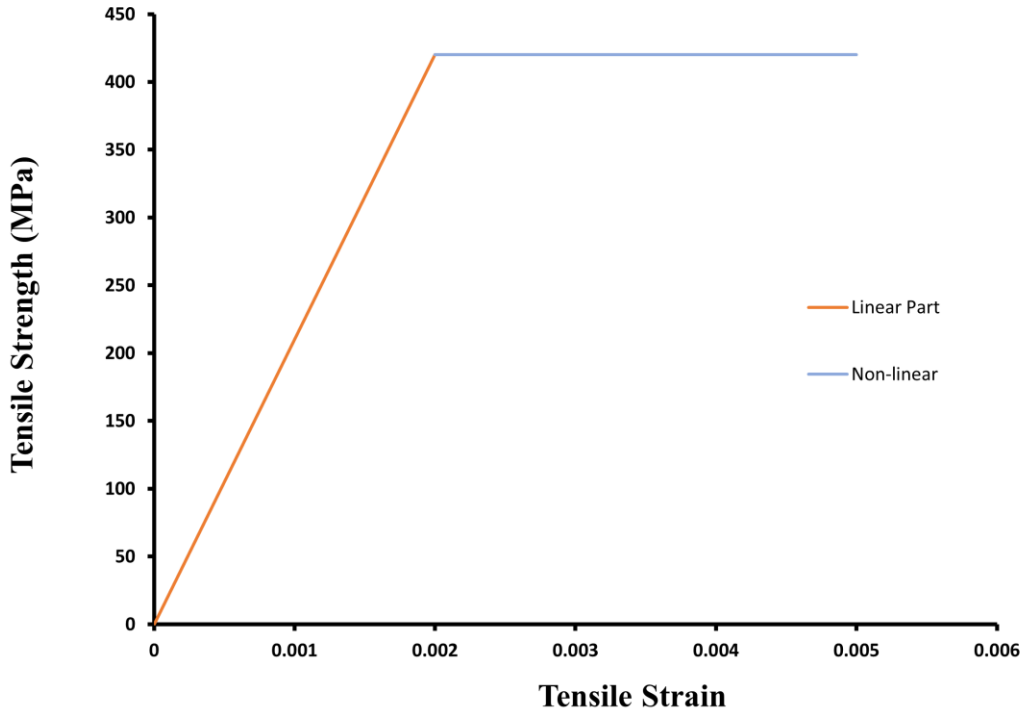

Figure 3.7 Tensile behaviour of steel reinforcement

3.3.3 FRP Plate

The materials properties of CFRP are modulus of elasticity (E_s), Poisson's ratio (ν), and tensile strength of CFRP. These materials' properties are provided in Table 3.3. The CFRP materials are assumed as perfectly elastic, as shown in Figure 3.8. In this thesis, the CFRP plate was modeled as isotropic instead of orthotropic because the load will be applied in the axial direction of the CFRP plate.

Table 3.3 Materials properties of CFRP plate

Materials Property	Value
Modulus of Elasticity ($\boldsymbol{E_s}$)	101 GPa
Poisson's Ratio ($\boldsymbol{\nu}$)	0.3
Ultimate Tensile Stress ($\boldsymbol{\sigma_t}$)	2066 MPa
Ultimate Tensile Strain ($\boldsymbol{\varepsilon_u}$)	1.56%

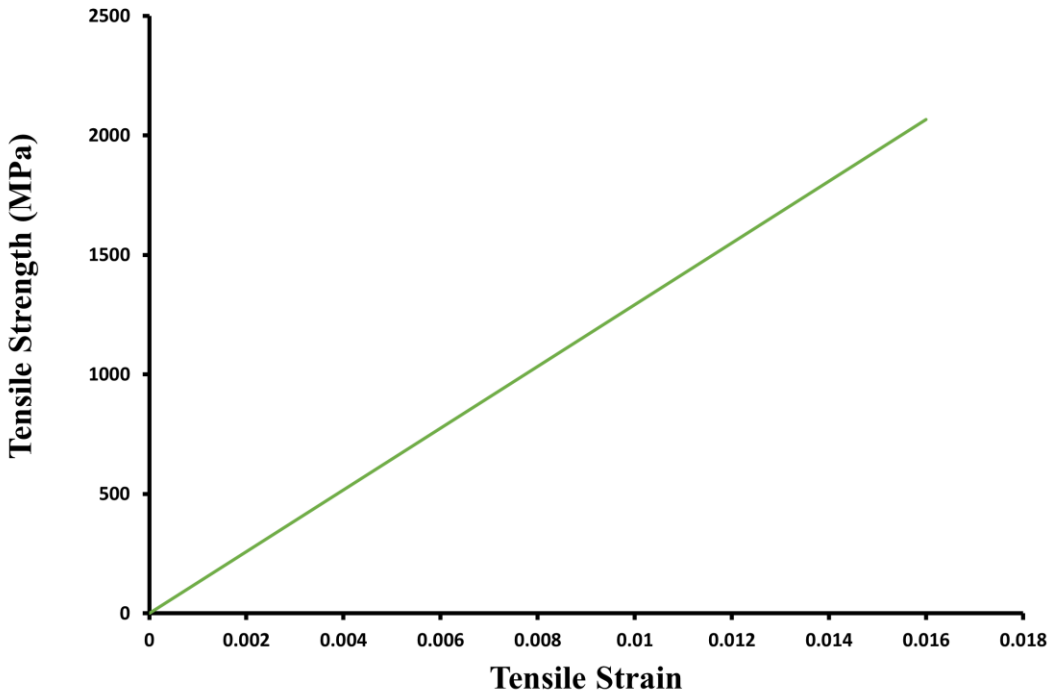

Figure 3.8 Tensile behaviour of CFRP

3.4Element Selection

The FEM provides the user with different types of elements to accurately simulate the response of each elements in modeling. To get the proper response, each element must be selected based on experimental characterizations. The main family types of elements that were used in this model were solid elements, truss elements, and shell elements as shown in Figure 3.9. As for elements order, there are two types, first and second order elements. In the first order elements, the nodes are placed in the corner only, and use linear interpolation to determine the output variables. In the second order elements, the nodes were not only limited to the corners and used different integration method which is quadradic integration. Even though second order elements have more accurate output values (results), it will cause convergence issue. So, the first order elements were used in this study.

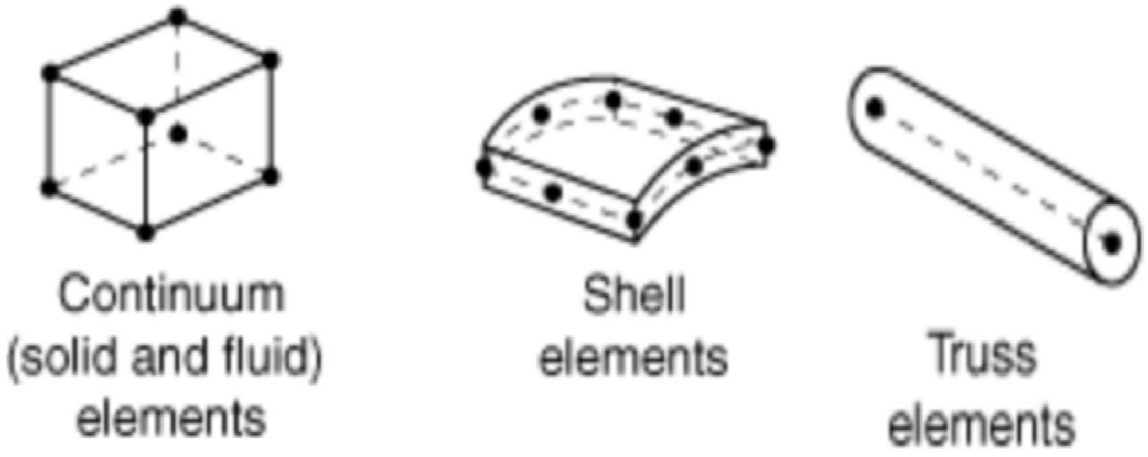

Figure 3.9 Elements in FEM (ABAQUS Documentation, 2010)

All of these elements have three degree of freedom in each node. Moreover, for all types of elements, there are two types of integration which are full or reduced integration. Reduced integration is defined to reduce the number points for each element which is different to full integration as presented in Figure 3.10. Reduced integration elements were used in the thesis to reduce computational time and avoid shear locking.

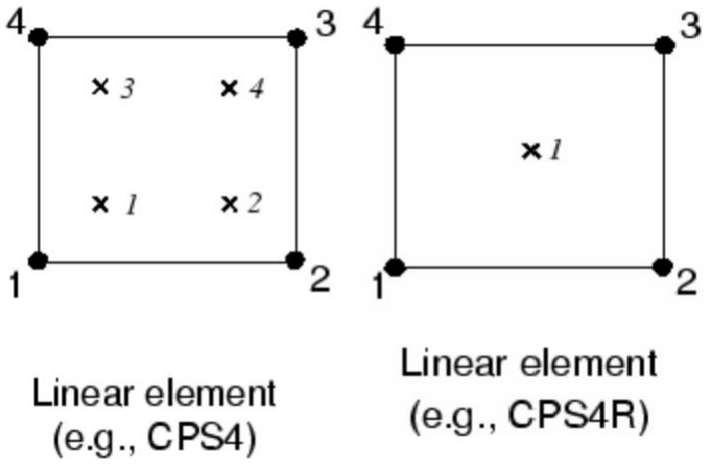

Figure 3.10 Full vs reduced integration elements (ABAQUS Documentation, 2017)

3.4.1 Continuum or Solid Element

The concrete part was modeled as continuum using solid elements in all simulations in these studies. In FEM, various types of solid element can be used to accurately represent the volume and geometric configuration of the model including tetrahedral, triangular prism, and brick as shown in Figure 3.11. These elements be linear or quadratic.

After carefully review different elements, the element that was chosen to represent concrete behaviour in this study is C3D8R where:

C Hexahedral continuum elements

3D Three dimensional

8 Eight nodes linear bricks

R Reduced integration

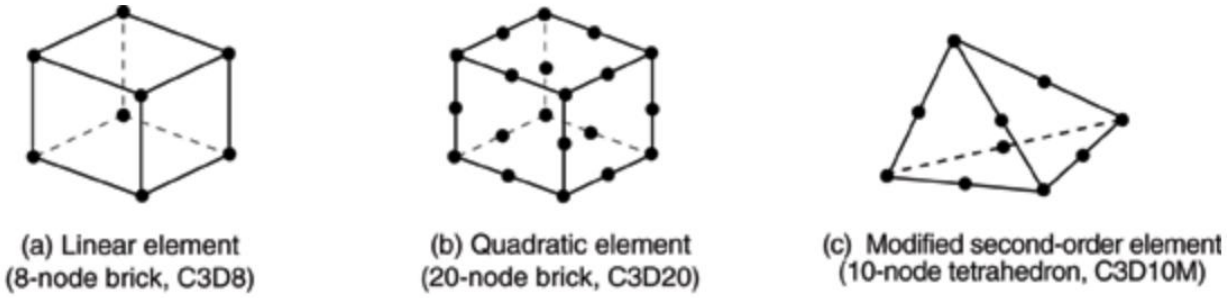

Figure 3.11Solid element with different number of nods (ABAQUS Documentation, 2011)

3.4.2 Truss Element

Main and transverse internal steel reinforcements were modeled as truss elements for all the analysis in this thesis. Truss element can be defined as slender element with two nodes as

shown in Figure 3.9. Besides, the truss element can carry only the axial force and cannot convey any moment or transfer load. In FEM, there are two types of truss element can be implemented to represent the behaviour of all the internal reinforcement including two nodes element and three nodes element as shown in Figure 3.12. The 2-node elements (T3D2) were used to all the internal main and transfer steel reinforcements where:

T Truss element

3D Three dimensional

2 Two nodes per linear element

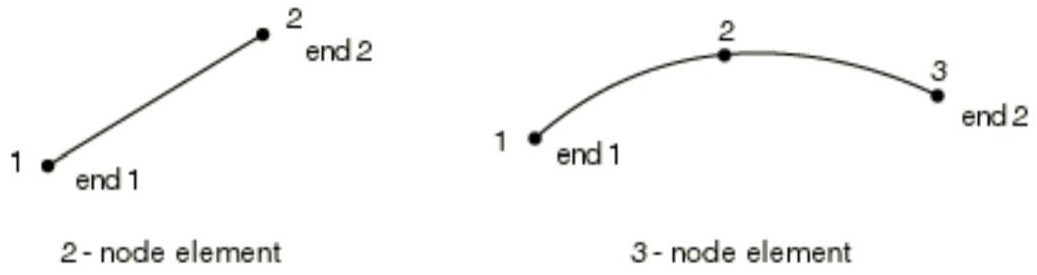

Figure 3.12 Truss elements with different number of nods (ABAQUS Documentation, 2017)

3.4.3 Shell Element

The third element type used in this study is the shell element to model the CFRP plate. The type of shell elements that was used in FEM is three-dimensional conventional shell elements. Shell elements were used to model the relatively thin CFRP plate, as shown in Figure 3.9. Furthermore, defining the surface direction is essential for shell elements due to small thickness which contributes to have orthotropic reaction under loading. In FEM, two types of shell element can be used to accurately represent the volume and geometric configuration of the model including

six nodes, and eight nodes element as shown in Figure 3.13. These elements can be linear or quadratic Therefore, S4R was used to mode the CFRP plate where:

S Shell element

4 Four nodes

R Reduced integration

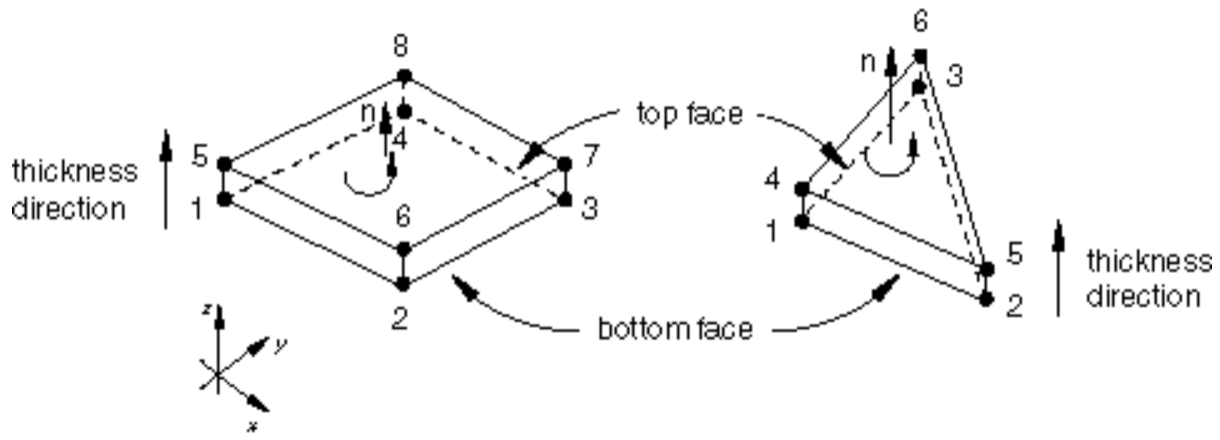

Figure 3.13 Shell element with different number of nods (ABAQUS Documentation, 2017)

3.5 Contact between Elements

Two contact surfaces were used in this model. The first surface is to model the embedded region of the internal steel reinforcement within the concrete. The second contact surface is to model the external contact between concrete and CFRP plate which were glued using epoxy. Both types of contacts are discussed in detail in section 3.5.1 and 3.5.2.

3.5.1 Contact between Concrete and Internal Reinforcement

Contact between concrete and internal steel reinforcements plays essential role in the accuracy of simulating the reinforced concrete sections. In this case, the bond will be created between concrete the internal reinforcements, ABAQUS has three different techniques which are:

1. Discrete technique: It can be used when the bond is formed by creating common nodes between the steel reinforcements, and concrete elements. However, this method is restricting the concrete mesh to the location of reinforcement's nodes.
2. Smeared elements method: In this technique the composite layers are used as bonding between steel reinforcements and concrete elements.
3. Embedded elements method: This method can be implemented by locating the embedded nodes on the host nodes.

The embedded elements method was used to model the contact between the concrete and steel reinforcement. In embedded elements method, host and embedded elements must be identified. To illustrate, concrete is represented as a host region while internal steel reinforcements are denoted as an embedded region. In this method, the nodes of embedded elements are aligned as nodes of the host region to constraint the translation degree of freedom of embedded nodes.

3.5.2 Interface between Concrete and CFRP Plate

Simulating the interface between the concrete and CFRP plate is the key to exhibit more precise and accurate solution. In this study, two types of modeling the interface were applied namely: perfect bond, and traction separation law. Firstly, perfect bond was used to simulate the bond behaviour between the concrete and CFRP plate when the failure is based on the rupture of CFRP plate. In that case, perfect bond shows a good agreement with experimental results; however, when the failure is caused by debonding the CFRP, perfect bond fails to capture the

separation. Secondly, cohesive modeling was used to simulate the delamination of CFRP plate by using the traction separation law. In the parametric studies, the cohesive modeling and failure by the maximum strain of the CFRP are considered because the mode of failure is unknown. So, the controlling failures were set in the FE model to be one of them (i.e., debonding, rupture of CFRP plate,) whichever happens first. The traction separation model was used with specified mechanical and geometric parameters to capture the failure of contact (Burlayenko & Sadowski, 2008). These parameters include initial stiffens (K_0), shear strength (τ_{max}), and fracture energy (G_f), as shown in Figure 3.14. The traction separation parameters can be expressed according to following equations (Obaidat, 2011):

$$K_{nn} = \frac{1}{\frac{t_c}{E_o} + \frac{t_{epoxy}}{E_{epoxy}}} \tag{3.15}$$

$$K_{ss} = K_{tt} = 0.16\ \frac{G_{epoxy}}{t_{epoxy}} + \ 0.47 \tag{3.16}$$

$$\tau_{max} = 1.46\ {G_{epoxy}}^{0.165} + \ f_{ct}^{1.033} \tag{3.17}$$

$$G_f = 0.52 f_{ct}^{0.26} + \ {G_{epoxy}}^{-0.23} \tag{3.18}$$

Where:

K_{nn} : the initial stiffens in normal direction in MPa.

$K_{ss} = K_{tt}$: the initial stiffens in tangential direction in MPa.

t_c : the concrete thickness in mm.

t_{epoxy} :the epoxy thickness in mm.

E_o : Young's modulus of concrete in MPa.

E_{epoxy} : Young's modulus of epoxy in MPa.

G_{epoxy} : Shear modulus of epoxy in MPa.

f_{ct} : the tensile strength of concrete.

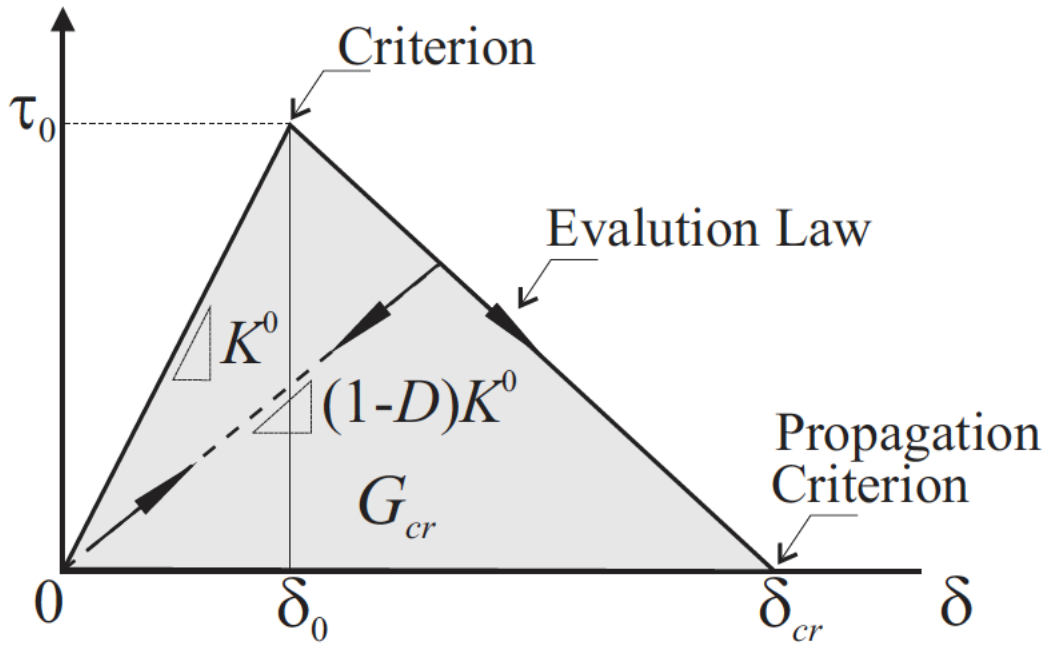

Figure 3.14 Bilinear traction separation law (Burlayenko & Sadowski, 2008)

3.6 Prestressing of CFRP Plate

Prestressed effects can be applied to the CFRP plate using FE models. In ABAQUS, there is an option of predefined field that allows the user to define any type of loading before any contact created with elements as shown in Figure 3.15a. Therefore, predefined field was used in this study

to apply prestressed on CFRP plate before its contact with concrete which simulates the real case of prestressing applied in the experimental test. To simulate prestressing properly, two steps were used in this study. In first step, the effect of prestressing was induced to CFRP plate by quasi static analysis as shown in Figure 3.15 b. The effect of prestressing was introduced by adding initial tension value that is equal to the level of prestressing applied in the experimental test. These levels were 5%, 20%, and 30% of ultimate tensile strength of the CFRP plate 2066 MPa uniformly distributed throughout the CFRP plate, as shown in Figure 3.15 b. In second step, the contact, boundary conditions, and loading were applied to simulate the stage of testing in the experimental test as shown in Figure 3.15c.

In modeling CFRP plate, the shell element was selected for this model. One of the most important aspect that must be considered in applying the effect of prestressing is defining the local coordinate system to select the proper direction of prestressing. This local coordinate system is defined by deciding the main axis, and transfer axis's as shown in Figure 3.16. In this thesis, the main axis (direction X) is aligned with the longitudinal direction of the CFRP plate and transfer directions are aligned with Y and Z axes representing width and thickness of CFRP plate, respectively.

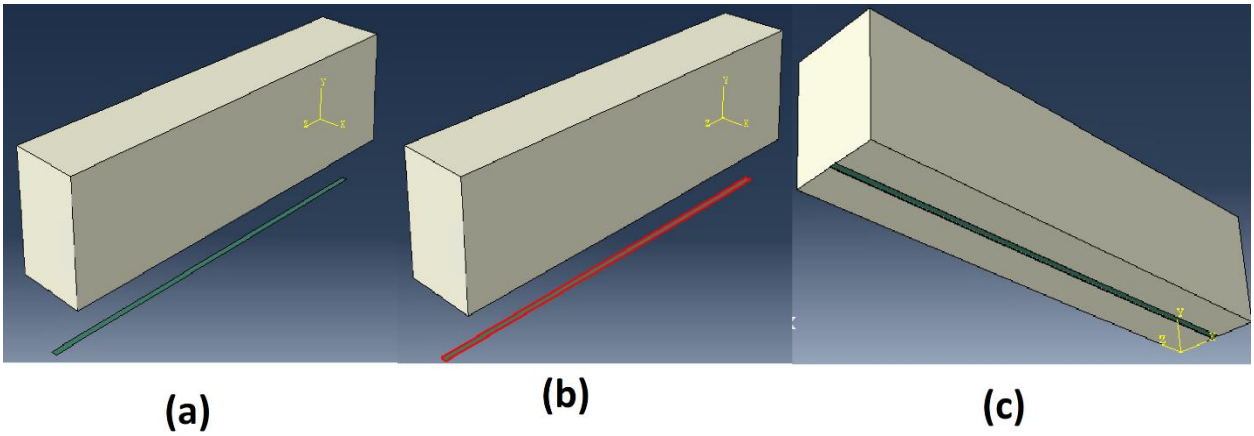

Figure 3.15 Process of applying prestressing on the CFRP plate

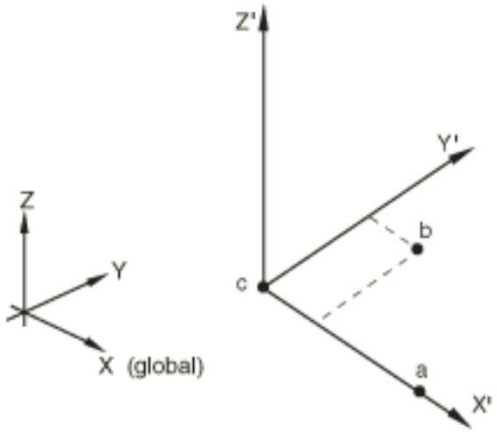

Figure 3.16 Local coordinate system (ABAQUS Documentation, 2011)

Since the most prominent failure modes of CFRP plate attached to concrete beam is debonding (peeling) of the plate of the concrete surface (Smith & Teng, 2002) (Yang et al., 2009) (Aram et al., 2008), the shear failure at the interface between the concrete and CFRP plate was applied, as shown in Figure 3.17. To illustrate, this debonding can be done by defining some failure criteria presented in section 3.5.2.

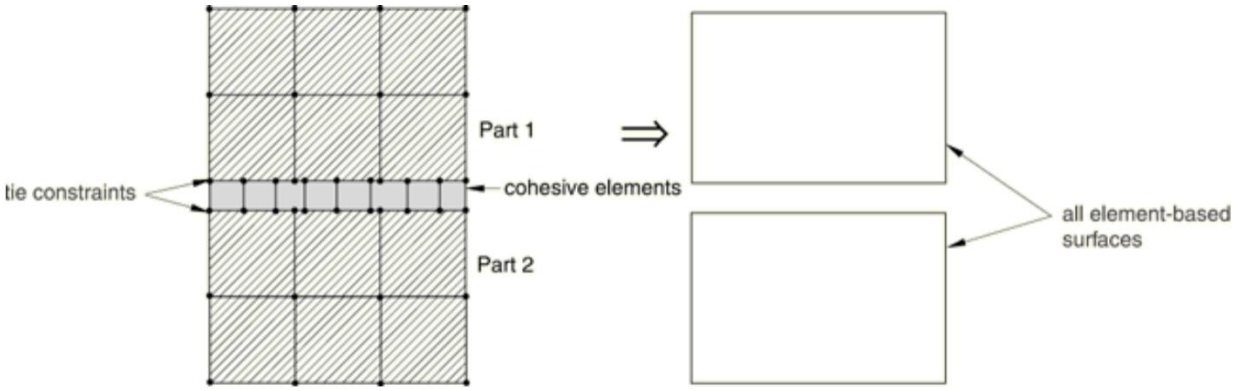

Figure 3.17 Bonding at nodes between concrete and CFRP plate (ABAQUS Documentation, 2017)

3.7 Boundary Conditions and Loading

Boundary conditions and loading used for modeling the prestressed CFRP plate with concrete are shown in Figure 3.18. For boundary conditions, in the experimental test, a simply supported beam were tested. Also, based of the symmetric configuration of the tested beam, only half of the beam was modeled. Therefore, to model the support conditions located at 150 mm from the ends of the beam as shown in Figure 3.16, displacement was restricted in directions X and Y, and represented by $U_2 = U_3 = 0$. On the other hand, the symmetry boundary condition was applied at the symmetry line located at 1650 mm as shown in Figure 3.16. They included the restriction of the movement in horizontal axis (directions Z), and the rotation about out of planes axis (direction X, and Y) represented by $U_3 = 0$, $UR_1 = 0$, and $UR_2 = 0$ respectively.

For loading, displacement-controlled loading was applied. To illustrate, a specific value of displacement was applied in the middle of the beam, this value was 90 mm to simulate three bending tests. To model these loading, allowable displacement was set to 90 mm in vertical axis (direction Y), $U_2 = -90\ mm$ and was located at 1650 mm as shown in Figure 3.18.

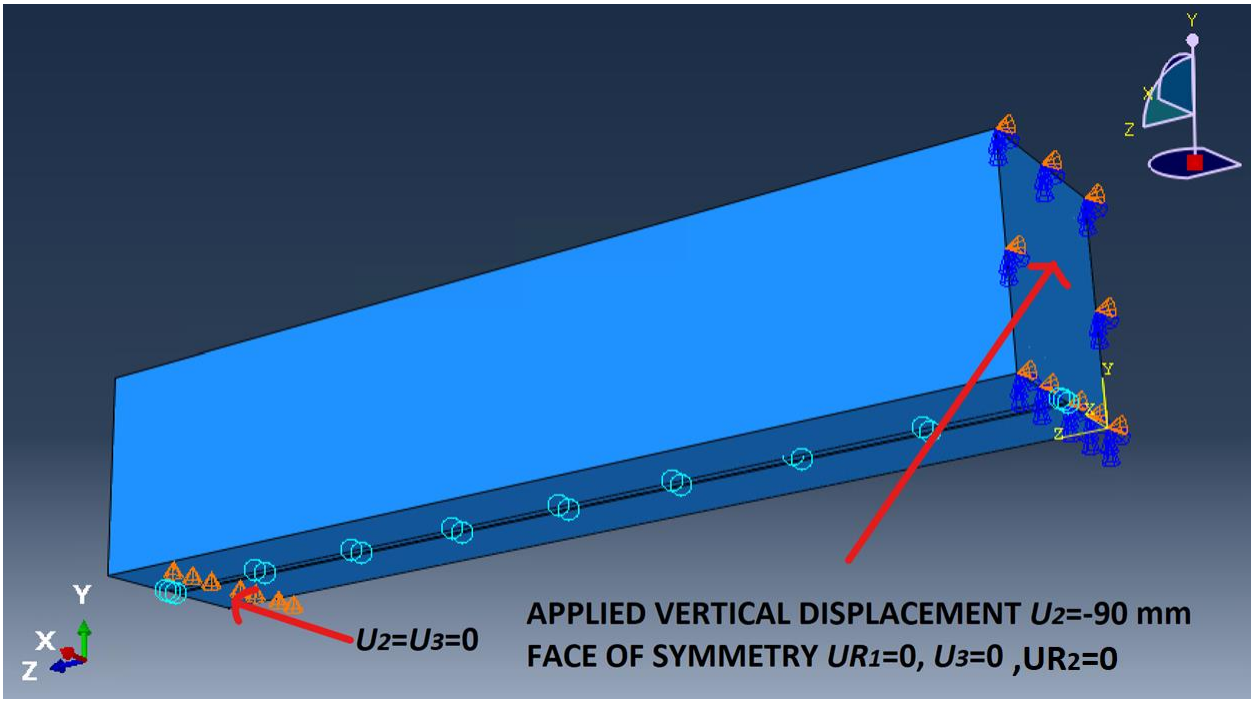

Figure 3.18 Boundary condition and loading

3.8 Meshing

Elements are varied as presented in 3.4 which results different meshing elements. The free meshing technique was used in this study. There are some steps must be followed to mesh any elements which are: deciding the number of seeds used in elements, and mesh order. Meshed of concrete beam is presented in Figure 3.19.

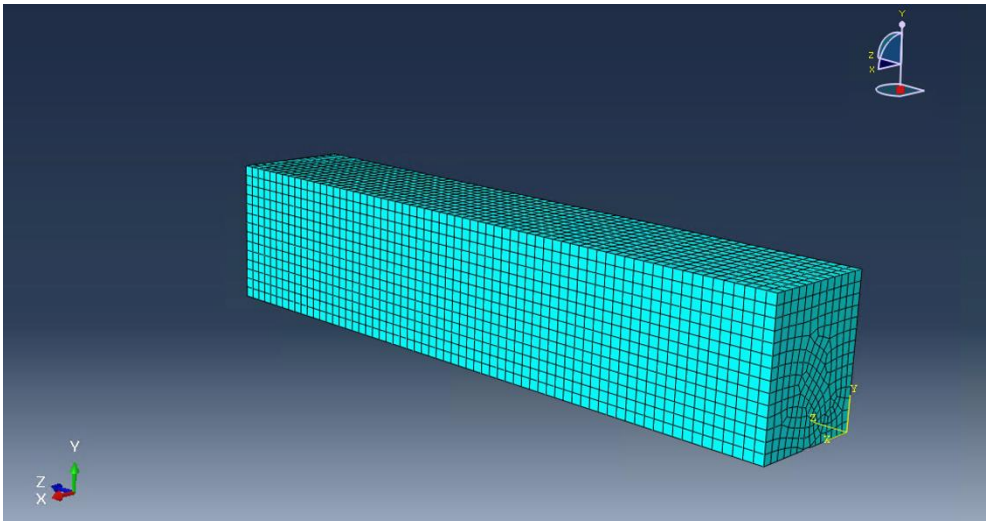

Figure 3.19 Meshing of concrete beam

Chapter 4: Results and Validations

4.1 Introduction

This chapter presents the results of the FE model. The calculated strength is presented and compared with the experimental results to determine the accuracy of the model. The differences are expected due to some errors associated with experimental tests. The plasticity modeling parameters of CDP were verified including the dilation angle (ψ) and viscoplastic regularization (μ). The numerical results for RC beams strengthened by CFRP plate with and without prestressing are presented and compared with the experimental results. Final recommendations in FE model's parameter are presented and applied in the parametric studies.

4.2 Verification of Models for Behaviour of Control RC Beam

Model verification was performed in this study to evaluate the validity of CDP models to represent an accurate behaviour of the control RC beam (without CFRP plate). The load-deflection relationship of control RC beam determined by FEM was compared with experimental one. The validation was applied by varying the dilation angle, viscosity parameter, and mesh refinement.

4.2.1 Dilation angle (ψ)

Dilation angle (ψ) is defined as the measure of change in volumetric strain with respect to the change in shear strain as shown in Figure 4.1 (Zhao & Cai, 2010). It was reported that as the dilation angle increases the ultimate strength predicated by the FE increases (Genikomsou, 2015).

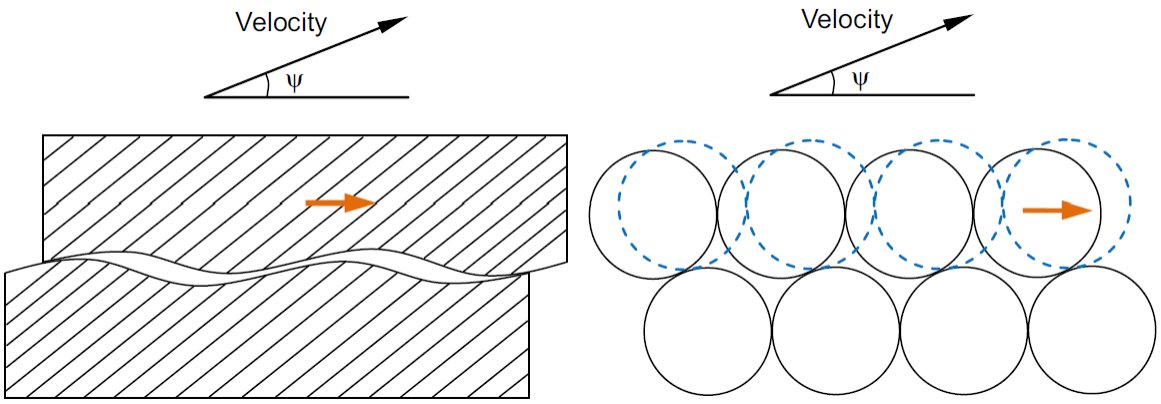

Figure 4.1 Dilation associated with sliding along microcracks and particles (Zhao & Cai, 2010)

As shown in Figure 4.2, increasing the dilation angles resulted in a slightly higher ultimate load value. In this thesis, 30° dilation angle was used for all models as recommended by Demin and Fukang (2017) for concrete materials. Other dilation angles were also investigated. For example, the value of 20° reduced the ultimate load by 2.5% while the value of 40° overestimated the ultimate load value by 2.2% (Mercan et al., 2010).

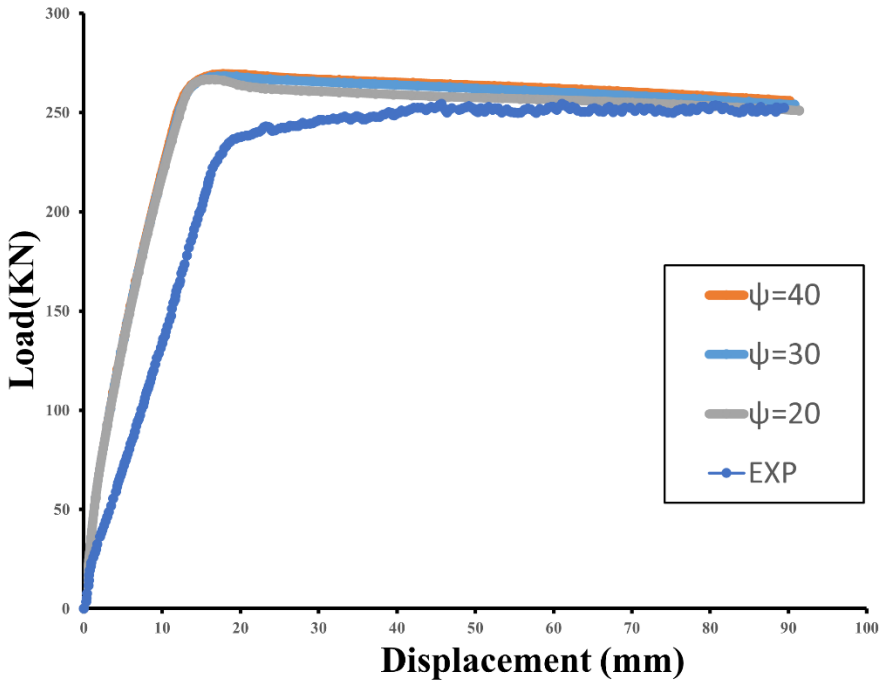

Figure 4.2 Influence of various dilation angle

4.2.2 Viscoplastic regularization

The viscoplastic regularization is defined by the value of viscosity parameter (μ) in the CDP model. Accurate viscosity parameter (μ) provides the model with more accurate results and reduces computation time. As shown on Figure 4.3, the value of $\mu = 0.001$ exhibited the most reasonable response for the concrete represented by the slope of the load-deflection curve that is similar to the experimental finding.

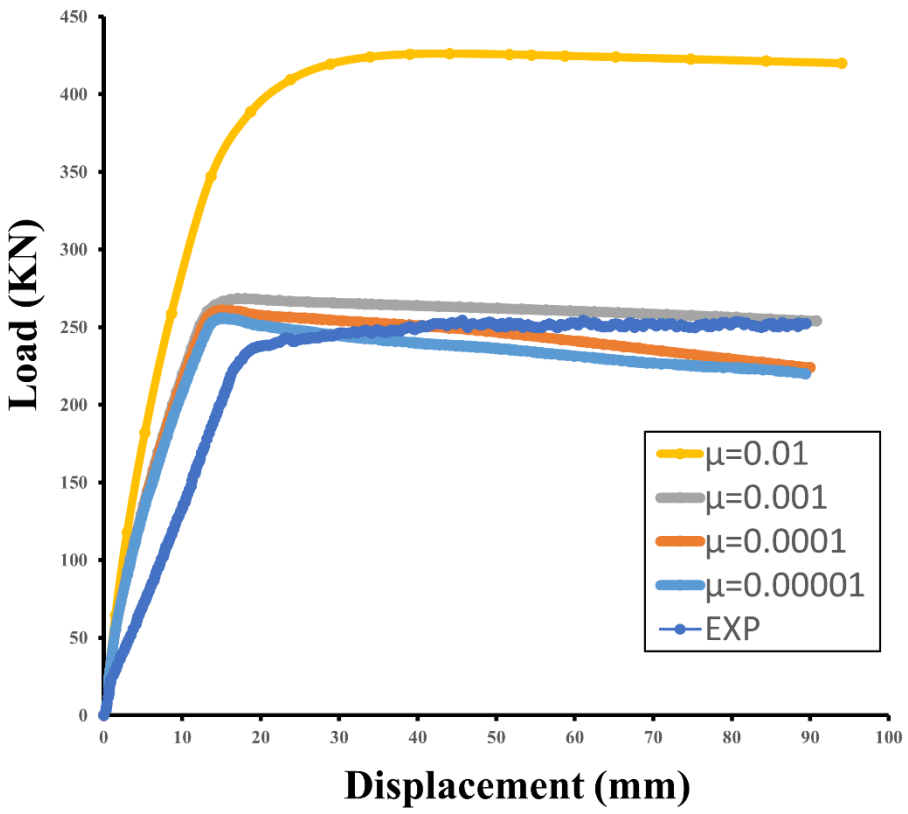

Figure 4.3 Influence of viscoplastic regularization

4.2.3 Mesh refinement

The influence of mesh density on all parts of concrete beam was investigated. Various mesh sizes were studied including 15,20, 25, 30, and 40 mm. Figure 4.4 illustrates the influence of mesh refinement in term of yield load. To change the mesh, seed size must be changed for each part in the model. However, finer mesh increases the computation time. After evaluating the effect of refinement of meshing, 25 mm (represented by the square point in the figure) was selected for this study as the results were stabilized at this size and smaller size of 15 mm and 20 mm element sizes. Moreover, 25 mm mesh size accurately captured the debonding between the RC beam and CFRP plate.

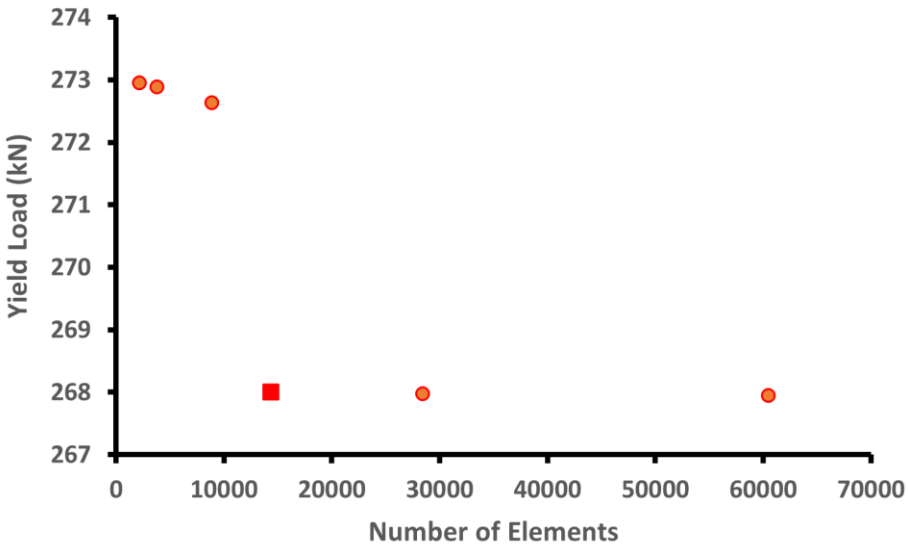

Figure 4.4 Influence of mesh refinement on yield load

4.3 Behaviour of Controlled RC Beam

The load versus deflection curve for control RC beams is presented in Figure 4.5. for both the experimental and FE model results. The calculated yield load, ultimate load, and deflection were compared with experimental results. Experimentally, the yield and ultimate loads were 233.2 kN and 254.8 kN, respectively. On the other hand, the FE results for yield and ultimate load were 268 kN and 253.93 kN, respectively. Consequently, the differences between the two results were 14.9% and 0.34% for the yield and ultimate load, respectively. For yield and ultimate deflection, the experimental result showed 17.65 mm and 89.5 mm for yield and ultimate deflection, respectively; however, the results of FE model indicated 15.2 mm for yield deflection and 90 mm for ultimate deflection. Therefore, the differences between them were 13.8% for the yield deflection and 0.55% for the ultimate deflection. In addition, the crack patterns recorded during the experimental tests were compared with the crack patterns obtained using FE model. This is done mainly by showing one of output variables which is the absolute plastic strain magnitude

(PEMAG) during analysis (Obaidat et al., 2010). The crack patterns obtained using FE and experimental for the RC beam are presented in Figure 4.6. It is shown that the FE models were generally able to capture the locations of the cracks in a similar manner obtained by the experimental testing especially in the middle of the beam that was controlled by the flexural loading. Overall, the result of the FE model is reasonably comparable to the experimental findings except at the yield load. One of the possible reasons for differences could be related to the perfect bond assumption between the internal steel reinforcement and the concrete used in the FE (Hawileh, 2012). However, applying other bond models makes the convergence of the model a challenging task (Hawileh, 2012) that is likely caused by the complication of slip-stick phenomenon when partial bond is applied.

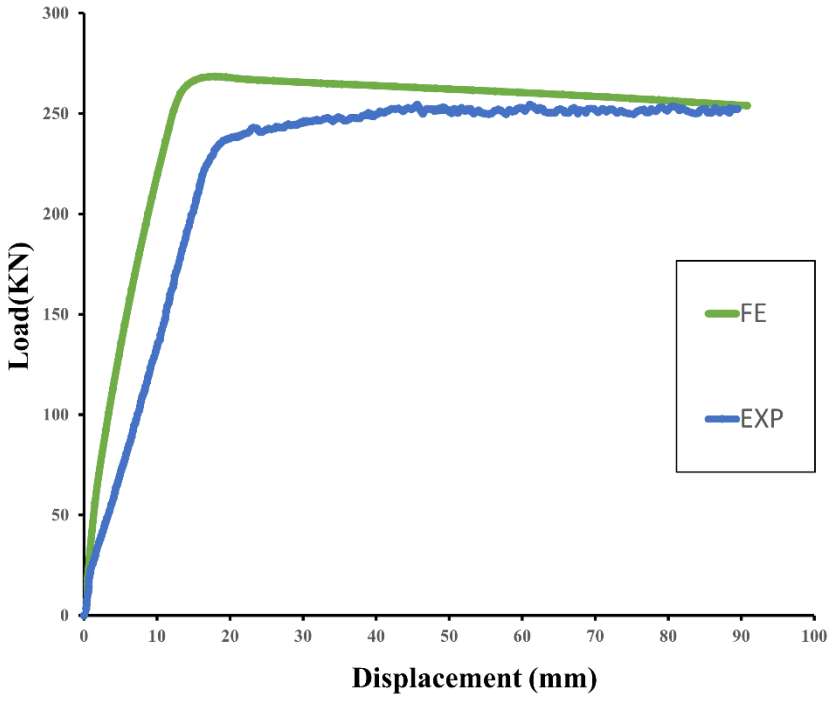

Figure 4.5 Load deflection curve of controlled RC beam

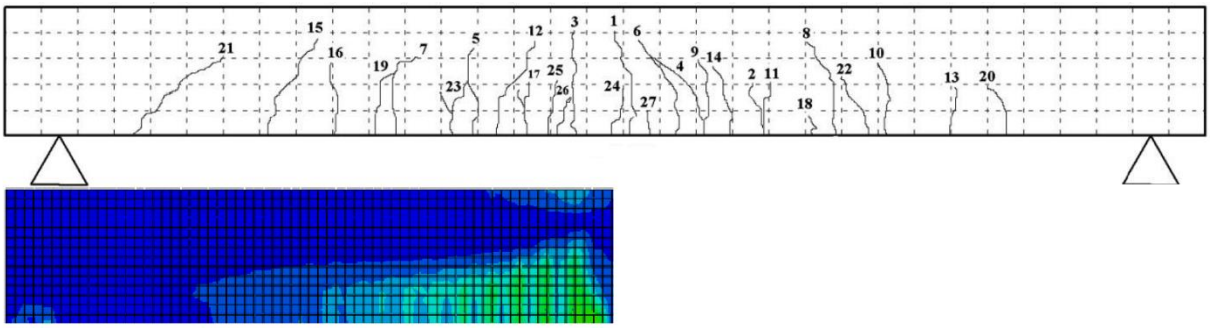

Figure 4.6 Crack patterns of experimental test vs FE

4.4 Behaviour of RC Beam Strengthened with Non-prestressed CFRP Plate

Strengthening RC beams with CFRP plate improved both the yield and ultimate load of the beams by attaching the CFRP plate to the tension side of the RC beam. For example, the ultimate load was enhanced by as much as 33% by applying non-prestressed CFRP plate to the RC beam (Obaidat et al., 2010). For the experimental results, the improvement was 1.42% and 10.6% for the yield load and ultimate load, respectively and the mode of failure was premature debonding of CFRP plate (Hajihashemi et al., 2011). This improvement was also captured by the FE models, as illustrated in Figure 4.7 that presents the load-deflection curves of both experimental test and FE model results. The yield and ultimate loads and corresponding deflections were used to compare between the results. Experimentally, the reported yield and ultimate load were 236.5 kN and 280.8 kN, respectively. However, the FE results showed that 272.2 kN for the yield load and 305.1 kN for the ultimate load representing the percentages of error of 15.1% and 8.65% for the yield and ultimate load, respectively. Also, the experimental yield and ultimate deflections were 17.8 mm and 82.86 mm, respectively. The calculated deflection using the FE model were 15.1 mm for the yield and 82.65 mm ultimate deflections representing the percentages of error of 15.1% and -0.25% for the yield and ultimate load, respectively. Furthermore, plastic strain magnitude

(PEMAG) as a representative for crack patterns obtained by FE model (Obaidat et al., 2010) was compared to the experimental one, as shown in Figure 4.8 . The FE accurately captured the mode of failure which is the debonding of CFRP plate, as one of the controlling failures set in the FE model (i.e. debonding, rupture of CFRP plate, whichever happens first). The debonding of the CFRP plate was modeled by reaching the shear strength of the interface while the rupture of CFRP was modeled by specifying a value of ultimate strain of the CFRP plate. Moreover, the general behaviour of the RC beam strengthened with CFRP plate is controlled by many factors including the ultimate tensile strength of the CFRP, and the number of used the CFRP plates, as reported by (El-Hacha & Rizkalla, 2004). According to El-Hacha and Rizkalla (2004) the enhancements of the yield and ultimate loads were 17.8%, and 16.1%, respectively by two CFRP strips with the ultimate tensile stress ($\boldsymbol{\sigma_t}$) of 1480 MPa. On the other hand, the yield and ultimate loads increased by 2.01 % and 33%, respectively for one CFRP plate with ultimate tensile strength of $\boldsymbol{\sigma_t} = 2640$ MPa) (Obaidat et al., 2010). The development of the yield and ultimate loads between the control specimen and strengthened one created by FE were 1.57%, and 11.34%, which are close to the experimental percentage for the same conditions that were 1.4%, and 10.2%. Based on the wide variation in the reported results for the ultimate load enhancement, the results of the proposed FE model lie within the reported results.

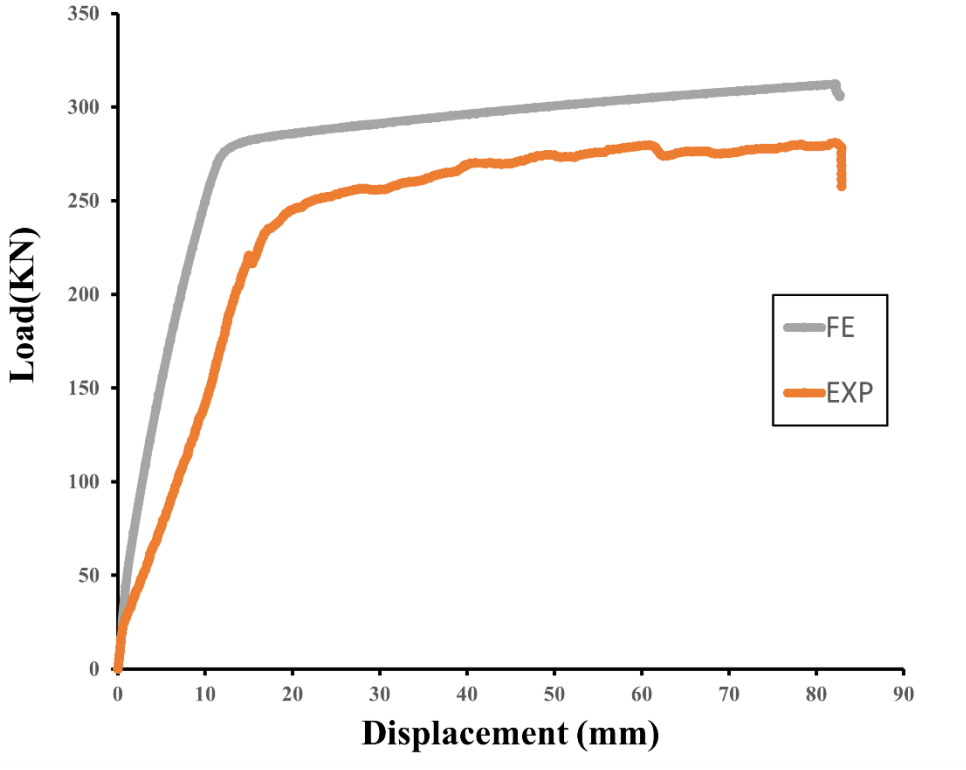

Figure 4.7 Load deflection curve of RC beam strengthened with CFRP plate

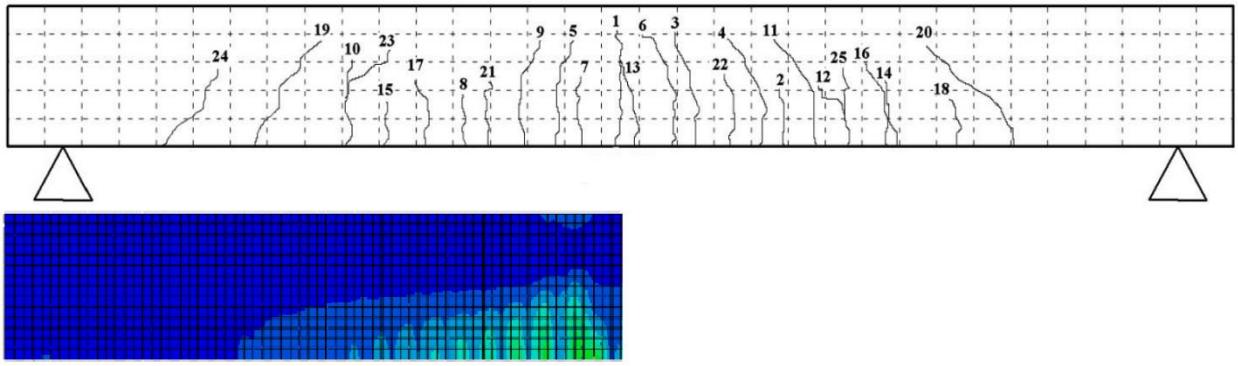

Figure 4.8 Crack patterns of experimental test vs FE

4.5 Behaviour of RC Beam Strengthened by Prestressed CFRP Plate

The prestressing of CFRP plate enhanced the performance of the RC beams as reflected by increased yield and ultimate loads. However, this performance enhancement is also accompanied by changing the modes of failure and challenges associated with gripping and attaching the prestressed CFRP materials to concrete that result in limiting prestressing level (up to 60%). Modelling prestressing levels of 5, 20, 30% used in experimental study under consideration is presented here whereas other prestressing levels will be presented in the next chapter.

4.5.1 Prestressing level of 5%

Increasing the prestressed level on the CFRP plate resulted in increasing the amount of stresses that transferred from the CFRP plate to RC beam which reduces the developed stresses in concrete and internal steel reinforcements resulting in improvement of load carrying capacity. To illustrate, increasing prestressing on the CFRP plate in strengthening RC beam improved the yield and ultimate loads by 77.2%, and 148.5 %, respectively compared to controlled RC beam (Yang et al., 2009). The experimental test for RC beams strengthened with prestressed 5% of CFRP plate showed improvement in the yield and ultimate loads by 5.06 % and 11.46%, respectively and the mode of failure was debonding of CFRP plate (Hajihashemi et al., 2011). The load deflection curve for both the experimental and FE model is presented in Figure 4.9. Both values of loads and deflections at the yield and ultimate were used to compare the FE and experimental results. The experimental results were 245 kN for the yield load and 284 kN for ultimate load, whereas for FE results were 275.8 kN and 311 kN for yield and ultimate load, respectively. The differences in the results for the yield load was 12.57% and for the ultimate load was 9.5%. The experimental results were 17.1 mm and 77.3 mm for the yield and ultimate deflections, whereas the yield and ultimate deflection using the FE model were 14.3 mm and 78.5 mm, respectively. For the deflection, the

percentages of changing between the FE model and experimental results were -16.4% for the yield deflection and 1.5% for the ultimate deflection. The crack patterns obtained by FE model and the experimental tests, were compared as shown in Figure 4.10. Both the crack patterns and the mode of failure were well represented by FE model. The improvement in yield and ultimate loads between the RC beam strengthened by non prestressed CFRP plate and 5% prestressed CFRP plate were 3.59%, and 1.14% which was close to the FE results of 1.32%, and 1.93%, respectively. Mostly, the ability of the FE model to represent the experimental load deflection, crack patterns, and mode of failure makes it a good tool to understand the general behaviour of RC beams. The main difference between FE and experimental results at the yield point can be attributed to the complexity of modeling interface between steel reinforcement and concrete as observed by (Ebead & Marzouk, 2005).

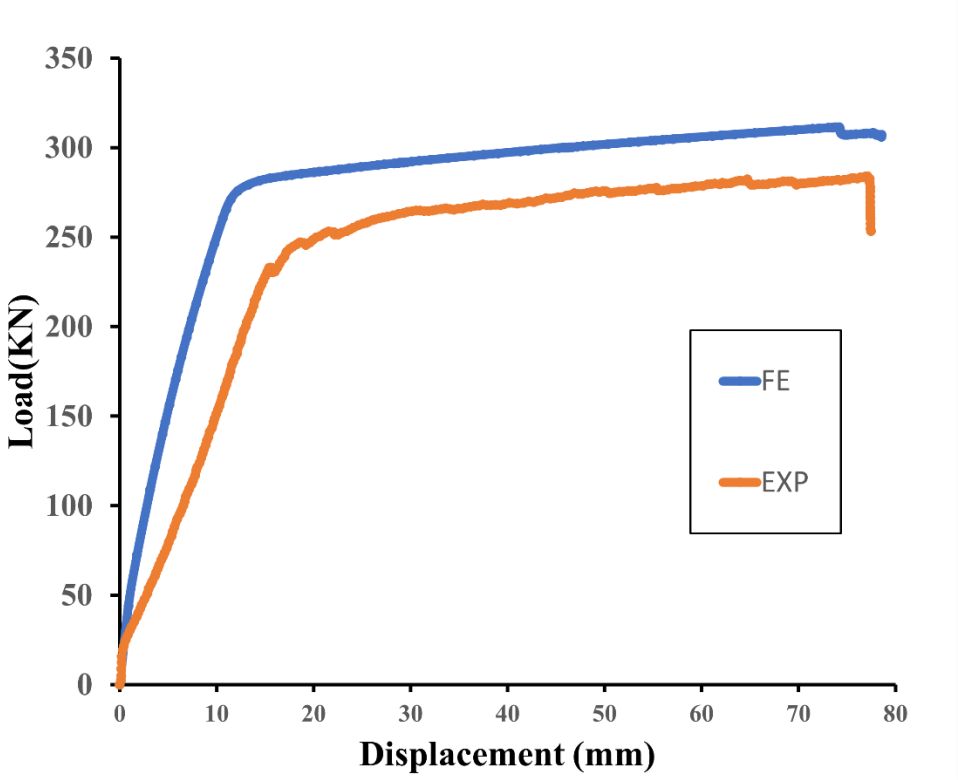

Figure 4.9 Load deflection curve of RC beam strengthened with prestressed (5%) CFRP plate

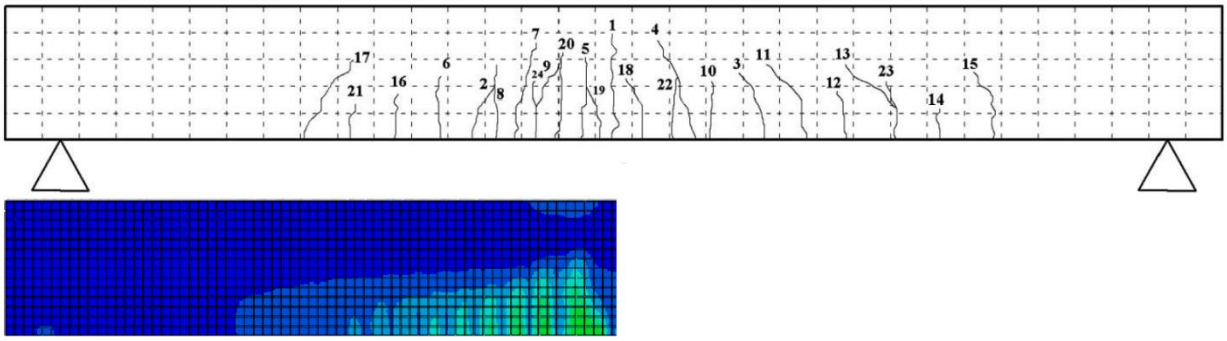

Figure 4.10 Crack patterns of experimental test vs FE

4.5.2 Prestressing level of 20%

Higher level of prestressing enhances the flexural response of strengthened RC beam, as reported in literature. For instance, increasing the prestressing level by 100% (from 20% to 40%) improved the yield and ultimate loads by 19%, and 1.85%, respectively (Yang et al., 2009). According to the experimental tests, strengthening the RC beam by CFRP plate that prestressed

with 20% enhanced both yield and ultimate load carrying capacity of controlled RC beams by 5.1% and 14.67%, respectively and the mode of failure was the rupture of the CFRP plate (Hajihashemi et al., 2011). Figure 4.11 presents the load deflection curve of experimental and FE results for RC beam strengthened with CFRP plate prestressed with 20%. To evaluate the efficiency of FE model, the results were compared with the experimental results for load carrying capacity and deflections. For load carrying capacity, the experimental values for yield and ultimate loads were 245.1 kN and 292.2 kN, respectively. The FE results were 279.2 kN and 315 kN for the yield and ultimate deflections, respectively. The variation between the FE and experimental results for the yield and ultimate loads were 13.91% and 7.8%, respectively. For the deflection, the yield value 16.3 mm and ultimate value 74.2 mm were recorded in the experimental tests, whereas the yield value of 13.9 mm and ultimate value of 72.6 mm were calculated for FE simulation. The gap between both results were -17.2 % and -2.15% for the yield and ultimate deflections. Furthermore, both the crack patterns as plastic strain magnitude (PEMAG) for FE model and experimental test results for strengthened RC beam with 20% prestressed CFRP plate are considered almost the same, as shown on Figure 4.12. The results obtained by FE for upgrading the yield and ultimate loads between RC strengthened with 5% and 20% CFRP plate were 1.23% and 1.29% while the upgrading of the experimental results were 0.04% and 2.89%, respectively which shows almost same experimental percentages in improvement for same conditions. Similar to the reported model of failure, rupture of the CFRP plate was observed in the FE as the failure mode. Generally, the result of the FE model is considered in good agreement with experimental results in term of load deflection curve, crack patterns, and mode of failures. However, the differences at the yield load between the FE model and experimental results is caused by using perfect bond between steel reinforcements and concrete (Ebead & Marzouk, 2005).

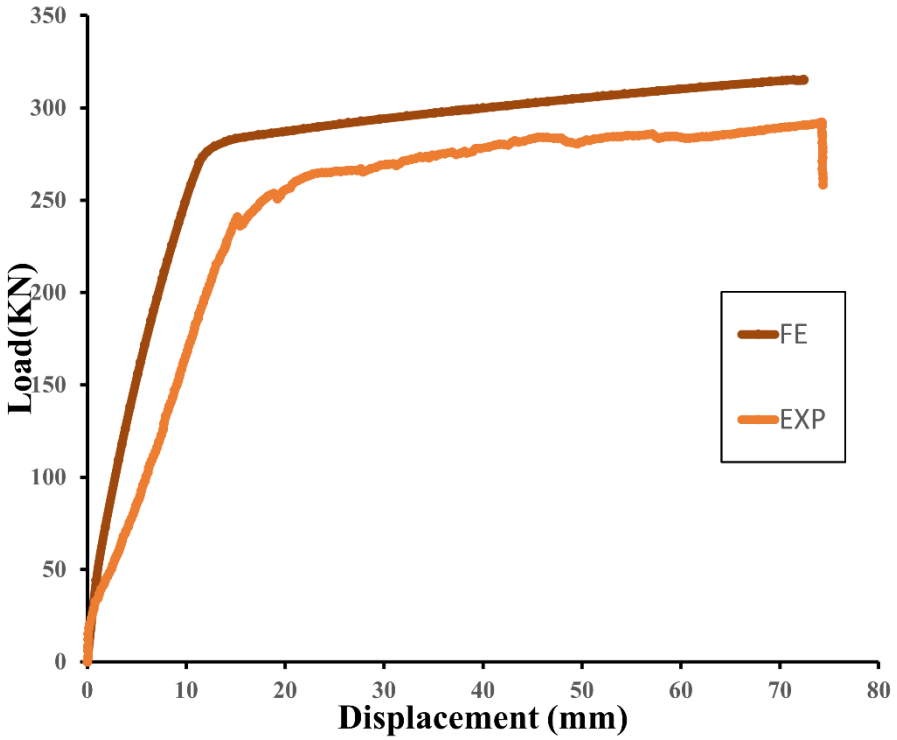

Figure 4.11 Load deflection curve of RC beam strengthened with prestressed (20%) CFRP plate

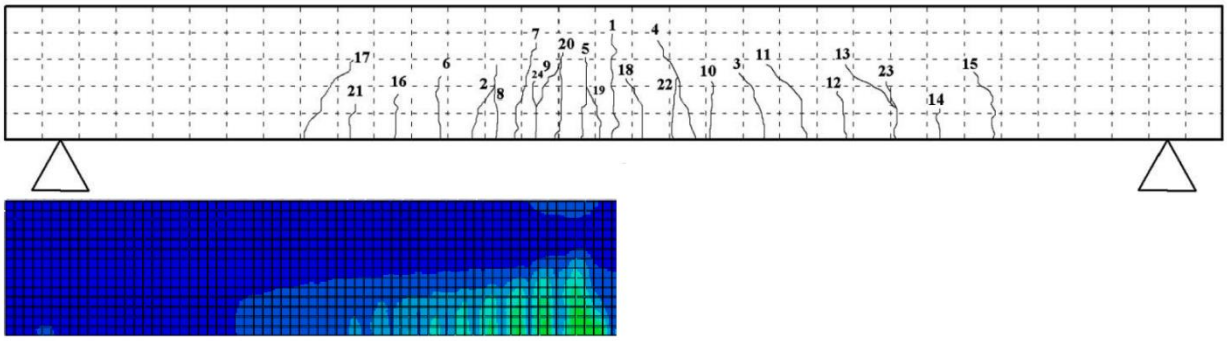

Figure 4.12 Crack patterns of experimental test vs FE

4.5.3 Prestressing level of 30%

Based on the experimental tests, strengthening the RC beam by further increasing prestressing level of CFRP plate from 20% to 30% showed an upgrading in both the yield load by 3.79% and the ultimate load by 0.27%, and the mode of failure was the rupture of CFRP plate (Hajihashemi et al., 2011).The typical load deflection curves for both experimental and FE results are shown in Figure 4.13. The yield and ultimate values for loads and deflections for the FE and experimental results were compared to verify the accuracy of FE model. For the loads, the experimental results were 254.4 kN and 293 kN for the yield and ultimate loads, respectively, on the other hand, the FE results were 279.83 kN and 317.28 kN for the yield and ultimate loads, respectively. The percentages of error were 10% for the yield load, and 8.29% for the ultimate loads. For the deflection, 16.1 mm, and 70 mm were the yield and ultimate values of deflection for experimental results, whereas the FE results were 13.4 mm, and 70.1 mm for the yield and ultimate deflections, respectively. The differences in the values between FE and experimental test were 20% and 0.1% for the yield and ultimate deflections, respectively. The crack patterns obtained by FE were in a good agreement with the crack patterns observed in the experimental results as shown on Figure 4.14. The enhancement on the ultimate loads by increasing the prestressing levels to 30% was 0.2% in the experimental results whilst the enhancement was 0.23% in the FE compared to prestressing by 20%. Mostly, the experimental load deflection curve, crack patterns, and failure mode were accurately represented by the result of FE model which contributed to consider the FE model as reliable. Nevertheless, the variation between the results of both FE model and experiments in term of yield load is mainly due to use the perfect bond between the internal reinforcement and concrete (Ebead & Marzouk, 2005). It is worth mentioned that further increase of the prestressing levels on the CFRP plate may trigger different flexural response of the RC

beams. Previous study showed that an increase in the yield and interestingly reduction in the ultimate loads by 18% and -1.92%, respectively by increasing the prestressing level from 40% to 60% (Yang et al., 2009). The main cause for the reduction in the ultimate load is the mode of failure which is the rupture of the CFRP plate. This gives important characteristics of the beam performance by applying higher prestressing of CFRP in strengthening applications.

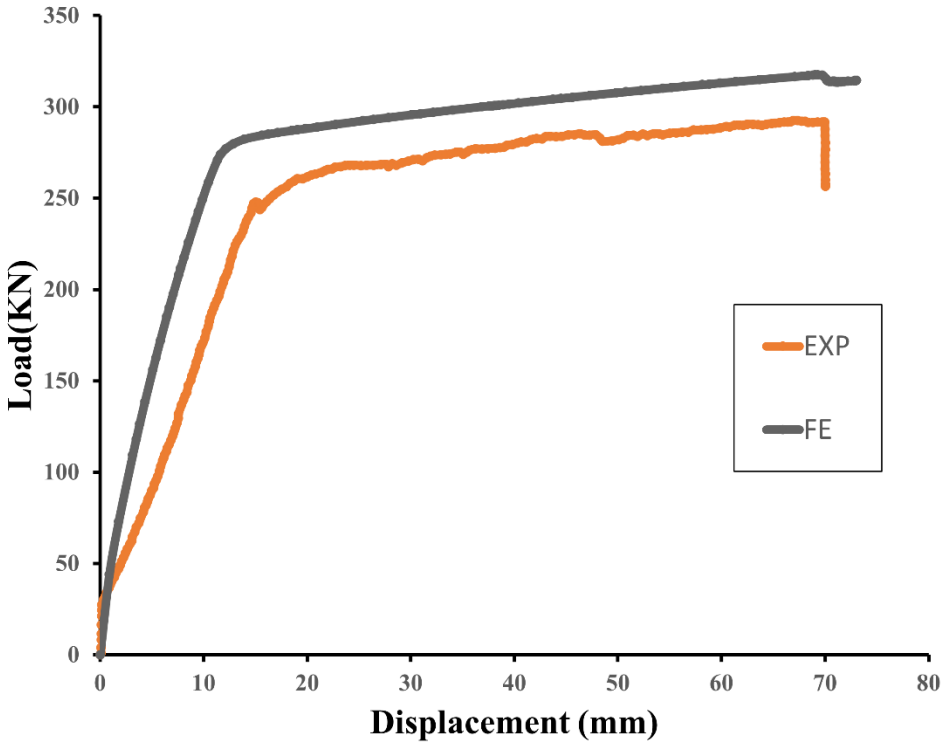

Figure 4.13 Load deflection curve of RC beam strengthened with prestressed (30%) CFRP plate

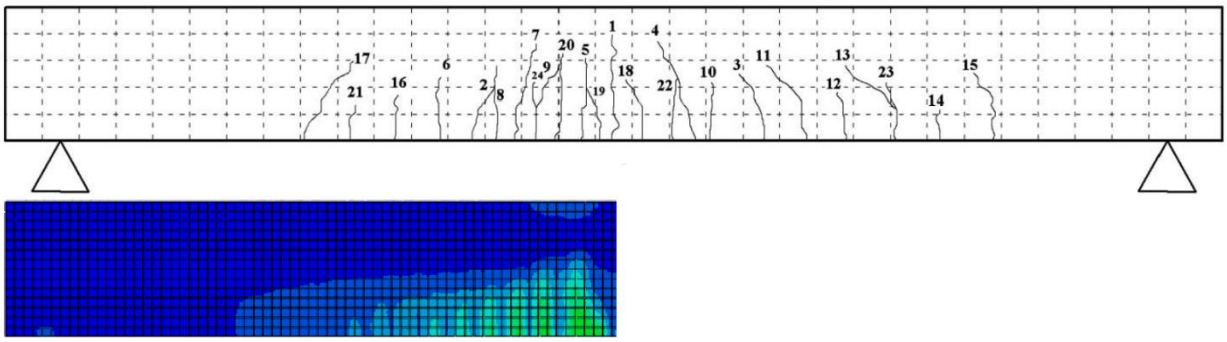

Figure 4.14 Crack patterns of experimental test vs FE

4.6 Comparison between FEM and Experimental Results for Yield Load

The load deflection curve can be divided into three phases: uncracked, cracked, and post yield. In the uncrack phase, the load increases linearly with increasing the deflection without any cracks. The second phase is defined when the load reaches the value of the load caused cracks to start to appear before reaching the yield load. In the cracked phase, the stiffness starts to decrease. The post yield phase, the value of the load at which the steel reinforcement yields, and the deflection starts to increase rapidly with little increase in the load (Azam, 2015).This different behaviour of RC between pre- and post-yield points emphasises the importance of yield load in investigating the flexural performance of RC beams. Consequently, a compression between the values of yield load using the experimental test and FEM is presented in Table 4.1. The FEM values for yield load are generally considered overestimated. For instance, the maximum overestimation was 15.1 % for the RC beam strengthened by CFRP plate, while the minimum overestimation was 10 % for RC beam strengthened with CFRP plate stressed by 30%.

Table 4.1 Summary of experimental vs FE results for yield loads

	Yield Load (kN)		
Specimen	**Experimental Load (kN)**	**FE result (kN)**	**Difference (%)**
Controlled RC beam	233.2	268	14.9
RC beam strengthened with CFRP plate	236.5	272.2	15.1
RC beam strengthened with prestressed CFRP plate (5%)	245	275.8	12.57
RC beam strengthened with prestressed CFRP plate (20%)	245.1	279.2	13.91
RC beam strengthened with prestressed CFRP plate (30%)	254.4	279.83	10

4.7 Comparison between FEM and Experimental Results for Ultimate Load

The ultimate load carrying capacity is one of the parameters normally used in investigating the flexural response of RC members specially, the ultimate load is affected by the failure modes such as debonding or rupture of CFRP plate. The values of ultimate loads were compared with the one obtained by FE model in Table 4.2. The comparison has indicated that the FE results have effectively estimated the ultimate loads. To illustrate, the most accurate percentage of error was 0.34 % for controlled RC beam, whereas the maximum overestimation was 9.5 % for RC beams

strengthened with prestressed (5%) CFRP plate. Furthermore, all the FE models were able to represents the failure modes in all of the investigated cases.

Table 4.2 Summary of experimental vs FE results for ultimate loads

	Ultimate Load (kN)		
Specimen	**Experimental Load (kN)**	**FE result (kN)**	**Difference (%)**
Controlled RC beam	254.8	253.93	0.34
RC beam strengthened with CFRP plate	280.8	305.1	8.65
RC beam strengthened with prestressed CFRP plate (5%)	284	311	9.5
RC beam strengthened with prestressed CFRP plate (20%)	292.2	315	7.8
RC beam strengthened with prestressed CFRP plate (30%)	293	317.28	8.29

4.8 Recommendations for Modeling RC and Prestressed CFRP Plate

Based on the calibration 99 models to accurately represent the experimental behaviour under the same conditions, recommended parameters are listed for all materials involved. The final parameters proposed for modeling the concrete and steel in RC beams are presented in Table 4.3, as well as table 4.4. Moreover, when CFRP are applied for strengthening RC beams, the proposed

parameters for CFRP plate the contact properties between RC beam and CFRP plate are presented in Table 4.5 and Table 4.6 respectively.

Table 4.3 Proposed parameters for modeling concrete

Parameter	Value or Type
Compression Model:	Hognestad Parabola
Tension Model:	Stress Strain Approach
Damage:	Compression and Tension
Poisson's Ration ($\boldsymbol{\nu}$)	0.2
Dilation Angle ($\boldsymbol{\psi}$)	30^0
Eccentricity	0.1
$\boldsymbol{f_{b0}/f_{co}}$	1.16
Viscosity Parameter(μ)	0.001
k	0.667
Mesh	25 mm

Table 4.4 Proposed parameters for modeling steel reinforcement

Parameter	Value or Type
Modulus of Elasticity ($\boldsymbol{E_s}$)	200 GPa
Poisson's Ration ($\boldsymbol{\nu}$)	0.3
Yield Stress ($\boldsymbol{f'_s}$)	423 MPa
Mesh	25 mm
Longitudinal Reinforcement	Truss Element

Stirrup Reinforcement	Truss Element

Table 4.5 Proposed parameters for modeling CFRP plate

Parameter	Value or Type
Modulus of Elasticity ($\boldsymbol{E_s}$)	200 GPa
Poisson's Ration ($\boldsymbol{\nu}$)	0.3
Ultimate Tensile Stress ($\boldsymbol{\sigma_t}$)	2066 MPa
Ultimate Tensile Strain ($\boldsymbol{\varepsilon_u}$)	1.6%
Mesh	25 mm
Element	Shell element

Table 4.6 Proposed parameters for modeling the contact between CFRP plate and RC beam

Parameter	Value or Type
Elastic Tensor ($\boldsymbol{K^0}$)	720 MPa
Cohesive Tensile stress ($\boldsymbol{\sigma_n}$)	1.81 MPa
Shear Strength in first direction ($\boldsymbol{\tau_n}$)	50
Shear Stress in second direction ($\boldsymbol{\tau_s}$)	50
Element	Cohesive Surface

4.9 Conclusions

The proposed models were evaluated based on the load deflection behaviour, and crack patterns, in addition to model of failure. Strengthening RC beam with CFRP plate, with and without prestressing, significantly improved the yield and ultimate loads. For the yield load, the percentages of error between FE and experimental results were 14.9%, 15.1%, 12.75%, 13.91%, and 10% for controlled RC beam, RC beam strengthened with regular CFRP plate, prestressed 5% CFRP plate, 20% CFRP plate, and 30% CFRP plate, respectively. For the ultimate load, the differences in the results of both the experimental and FE were 7.54%, 8.65%, 9.5%, 7.8%, and 8.29% for controlled RC beam, RC beam strengthened with regular CFRP plate, prestressed 5% CFRP plate, 20% CFRP plate, and 30% CFRP plate, respectively. This variation was expected given the vast number of parameters that affect the performance of RC beam in the FE and experimental investigations. Finally, the proposed models will be used for the parametric study on the next chapter.

Chapter 5: Parametric Study

5.1 Introduction

This chapter presents the parametric study to investigate some factors that may have an impact on the flexural behaviour of RC beams strengthened with prestressed CFRP plate. These factors include the prestressing level of the CFRP plate, and yield stress of steel reinforcement (f_s'). Also, the effects of CFRP plate geometric characteristics (length, width, and thickness) were also investigated. These parameters were selected because of their expected impact on the flexural behaviour of beams (Obaidat, 2011), in addition to the rehabilitation cost associated with the used amount of CFRP.

5.2 Effect of Prestressing Level

A parametric study was performed to investigate the effect of increasing the prestressing levels on the performance of the RC beams strengthened with CFRP plate. These prestressing levels were represented as a percentage of the ultimate tensile strength of the CFRP plate (i.e., 2066 MPa). Different prestressing levels of CFRP 40%, 50%, and 60% were investigated experimentally using similar range reported in literature (Yang et al., 2009). It was reported that increasing the prestressing level from 0% to 20% for CFRP plate increased the yield and ultimate loads of the RC beams by 77.2%, and 148.5 %, respectively compared to the control RC beam. Also, increasing the prestressing level of the CFRP plate by 100% (i.e., 40% level) improved the yield, and ultimate loads of the control beams by 19%, and 1.85%, respectively compared to strengthening with 20% prestressed CFRP plate. Similarly, higher prestressing level of 60% enhanced the yield, and ultimate loads by 18%, and -1.92%, respectively compared with RC beam strengthened by 40% prestressed CFRP plate. The load deflection curve for RC beam strengthened

by different prestressed levels of CFRP plate (0%, 5%, 20%, 30% 40%, 50%, and 60%) is shown on Figure 5.1. Generally, increasing prestressing levels of CFRP plate improved the load carrying capacity of RC beam between 20.13% to 20.95% for the yield load and 13.99% to 15.03% for the ultimate loads as shown on Table 5.1.The minor improvement on the yield load by increasing the prestressing level was noticed in the experimental tests too. Also, the modes of failure were the rupture of CFRP plate with higher levels of prestressing.

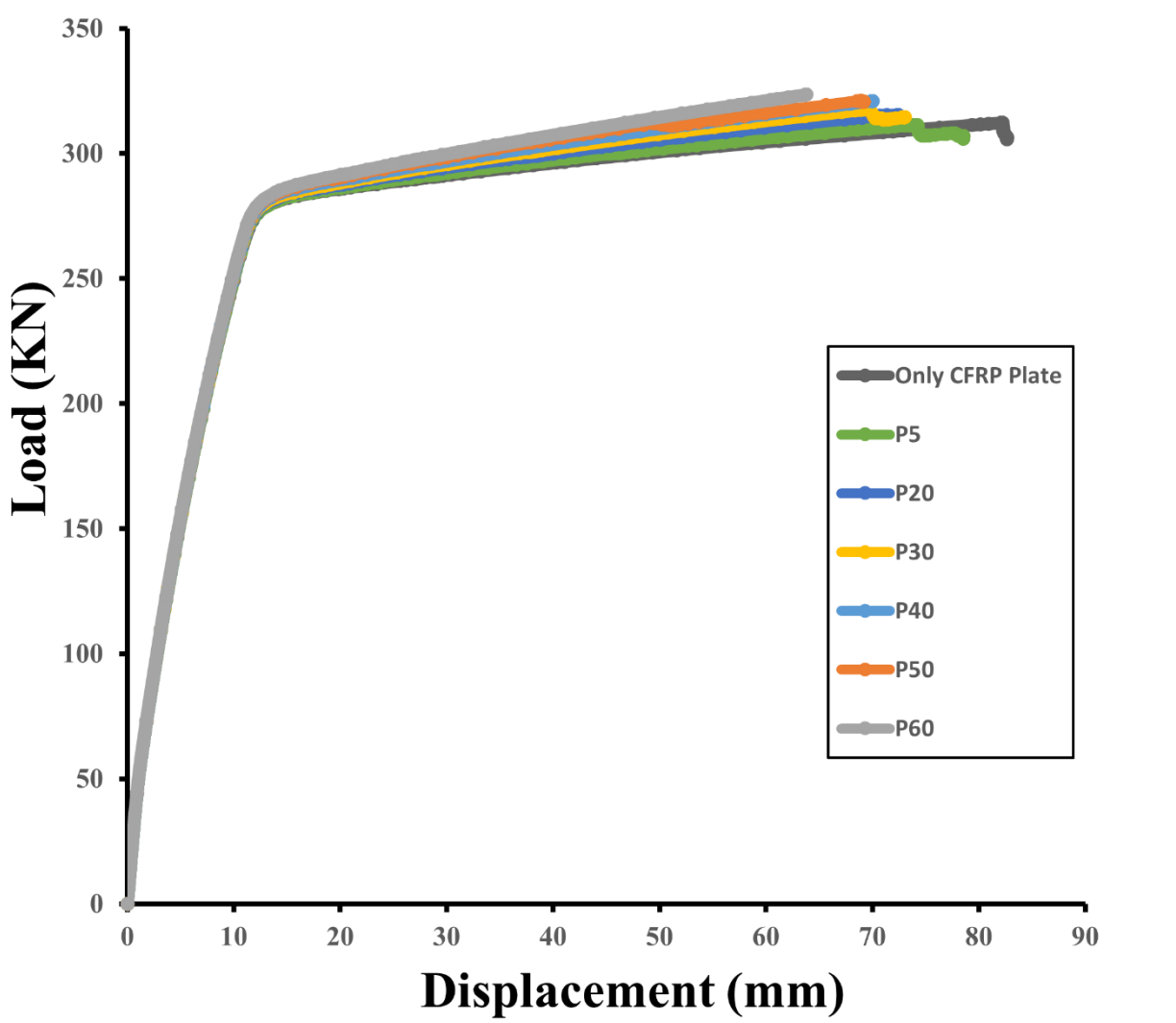

Figure 5.1 Effect of prestressing levels of CFRP plate

Table 5.1 Effect of prestressing levels of CFRP plate

Prestressing Levels	Yield Load (KN)	Increase in Strength (%)	Ultimate Load (KN)	Increase in Strength (%)
40%	284.1	20.13	320.1	13.99
50%	284.57	20.32	320.7	14.21
60%	285.2	20.59	323	15.03

5.3 Effect of Steel Strength

The effect of using higher grades of steel reinforcements on the flexural behaviour of strengthened RC beams with different prestressing levels of CFRP plate were conducted. Three grades of steel reinforcement with various yield stresses (f_s') including 500 MPa, 580 MPa, and 590 MPa were used on this study (Tavio et al., 2018), in addition to the regular steel of 423 MPa. Increasing the steel strength from the regular steel of 423 MPa to 500 MPa increased the yield loads by 36.3%, 37.9%, and 38.17% for RC beam strengthened with CFRP plate prestressed with 5%, 20%, and 30%, respectively compared to regular steel grade (423 MPa) for the same prestressing levels on the CFRP plate. Increasing the steel strength again to 580 MPa improved the yield loads by 47.6%, 50.1%, and 51.4% for RC beam strengthened with various prestressing levels of 5%,20%, and 30%, respectively with respect to regular steel grades for the same prestressing levels on the CFRP plate. Similarly, increasing the steel strength to 590 MPa increased the yield loads by 50.8%, 54.9%, and 55.2% for RC beam strengthened with prestressed CFRP plate with 5%,20%, and 30%, respectively compared to regular steel grades for the same prestressing levels on the CFRP plate. The effect of reinforcing steel strength on the yield loads of beams with respect to the regular steel grade are presented on Figure 5.2.

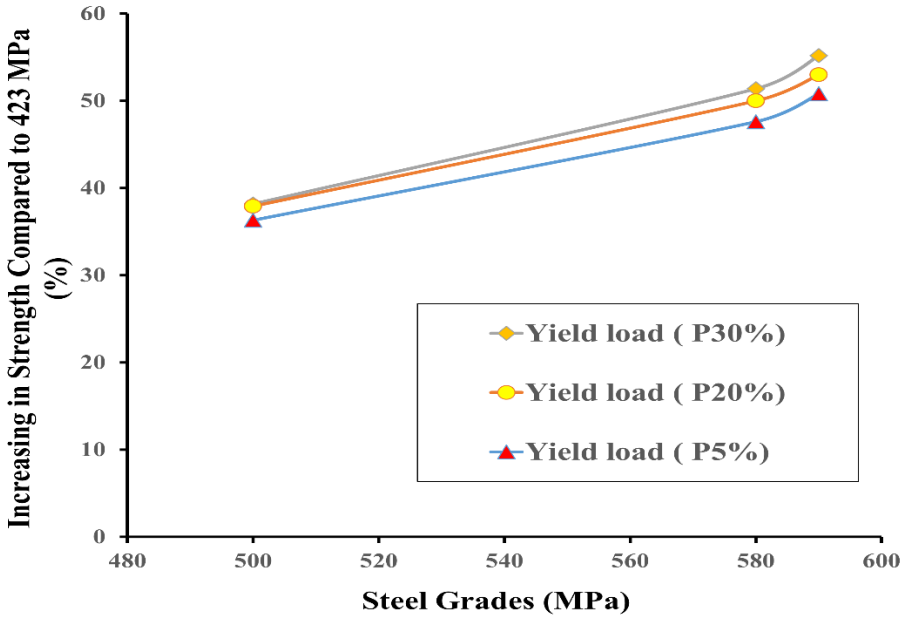

Figure 5.2 Increasing in the flexural strength of retrofitted RC beam (%) vs steel grades (MPa) for yield loads with respect to the regular steel grade of 423 MPa

Increasing the steel strength to 500 MPa increased the ultimate loads by 47.7%, 48.9%, and 49.8% for RC beam strengthened with CFRP plate prestressed with 5%, 20%, and 30%, respectively compared to regular steel grades for the same prestressing levels on the CFRP plate. Increasing the steel strength again to 580 MPa improved the ultimate loads by 62.5%, 64.4%, and 67.1% for RC beam strengthened with prestressed CFRP with various values 5%,20%, and 30%, respectively regarding regular steel grades for the same prestressing levels on the CFRP plate. Ever-increasing the steel strength to 590 MPa developed the ultimate loads by 64.2%, 66.1%, and 69.3% for RC beam strengthened with prestressed CFRP with 5%,20%, and 30%, respectively compared to regular steel grades for the same prestressing levels on the CFRP plate. The change in the ultimate loads regarding various steel grades with regard to regular steel grade for the same prestressing levels on CFRP plate are presented on Figure 5.3. Moreover, the change in the yield

and ultimate loads regarding various steel grades regarding regular steel grade are presented on Table 5.2.

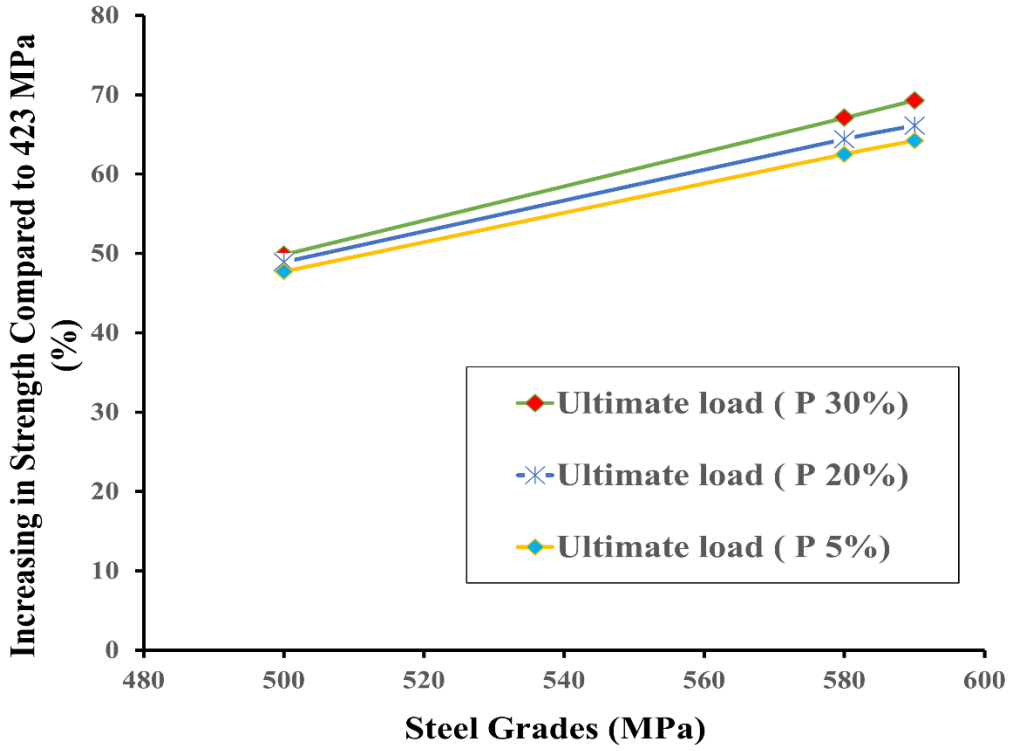

Figure 5.3 Increasing in the flexural strength of retrofitted RC beam (%) vs steel grades (MPa) for ultimate loads with respect to the regular steel grade of 423 MPa

Table 5.2 Effect of steel grade on retrofitted RC beam with various prestressing's levels of CFRP plate

Steel Grade	Prestressing Level (%)	Yield Load (KN)	Increase in Strength (%)	Ultimate Load (KN)	Increase in Strength (%)
500 MPa	5	334	36.3	362	47.7
	20	338	37.9	365	48.9
	30	340.4	38.17	372	49.8
580 MPa	5	361.7	47.6	398.2	62.5
	20	373.3	50	402.9	64.4
	30	373.8	50.12	410	67.1
590 MPa	5	369.4	50.8	402.3	64.2
	20	379.8	54.9	407	66.1
	30	381.9	55.2	415.5	69.3

According to the results, increasing the steel strength would gradually improve the load carrying capacity of RC bean strengthened with different levels of prestressing CFRP plate. Mainly this improvement is due to the additional resistance provided by higher yield stress of steel reinforcement.

5.4Effect of the Length of Prestressed CFRP Plate

The effect of different lengths of prestressed CFRP plate in strengthened retrofitted RC beams were investigated in this study since the length of CFRP has significantly affected the strengthening's level as reported by (Obaidat et al., 2010) and presented on Table 5.3. Decreasing the CFRP length to the half from 3300 mm to 1650 mm reduced the yield load by 0.035%, 0.23%, and 0.18% for various prestressing levels 5%, 20%, and 30%, respectively. Decreasing the CFRP

length further from 1650 mm to 550 mm lowered the yield load by 0.2%, 0.36%, and 0.21% for 5%, 20%, and 30% prestressing levels, respectively. Reducing the CFRP plate's length again from 550 mm to 412.5 mm decreased the yield load by 0.24%, 0.4%, and 1.33% for various prestressing levels 5% ,20%, and 30%, respectively. Reducing the length of CFRP plate from 3300 mm to 1650 mm decreased the ultimate load by 0.61%, 0.59%, and 0.37% for various prestressing levels 5%, 20%, and 30%, respectively. Decreasing the length again from 1650 mm to 550 mm reduced the ultimate loads by 3.63%, 3.73%, and 4.95%, respectively. Further reduction of the length from 550 mm to 412.6 mm decreased the ultimate load by 7.65%, 8.73%, and 9.1% for 5%,20%, and 30% prestressing levels, respectively. Figure 5.4 shows the effect of different length of CFRP prestressed (5%) on retrofitted RC beam.

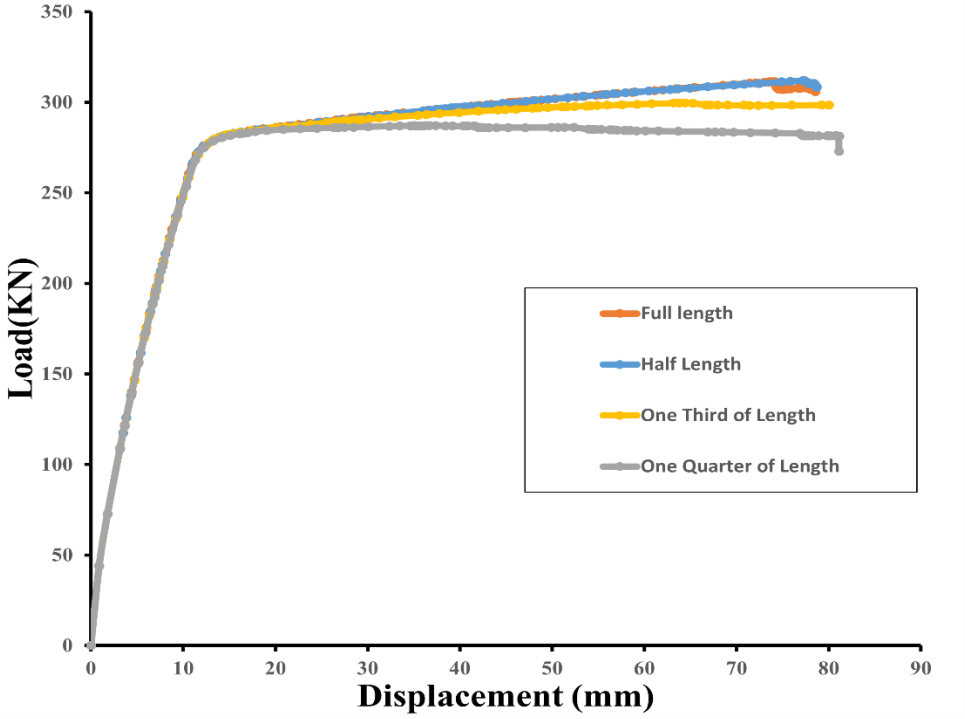

Figure 5.4 Effect of different length of prestressed (5%) CFRP plate

Table 5.3 Effect of different length of CFRP plate

Prestressing Level (%)	Length of CFRP Plate (mm)	Yield Load (KN)	Decrease in Strength (%)	Ultimate Load (KN)	Decrease in Strength (%)
5	3300	275.8	_	311	_
	1650	275.71	0.03	309.1	0.61
	550	275.24	0.2	299.7	3.63
	412.6	275.13	0.24	287.2	7.65
20	3300	279.2	-	315	-
	1650	278.55	0.23	313.13	0.59
	550	278.2	0.36	299.4	3.73
	412.6	278.1	0.4	287.5	8.73
30	3300	279.83	-	317.28	-
	1650	279.32	0.18	316.1	0.37
	550	279.24	0.21	301.56	4.95
	412.5	279.1	1.33	288.4	9.1

According to the results, decreasing the length of the CFRP plate has an influence on the flexural behaviour of retrofitted RC beam especially on the ultimate loads carrying capacity, but little effect on the yield capacity. The reason for the little enhancement in yield load is that the yield occurred at the mid-span of the beam which was already covered by the CFRP plate of any length. This effect is primarily due to the additional resistance obtained by longer length of prestressed CFRP plate. Moreover, there was a minor improvement on the yield loads when increasing the level of prestressing on the CFRP plate such results were noticed when the

prestressing increased on the experimental tests from 0% to 30% (Hajihashemi et al., 2011). However, for strengthening with full and half length of CFRP plate development noticed on the ultimate loads was almost the same. This similarity on percentage of strengthening was mainly due to covering more than of 25% shear span (almost 50% of the length of the RC beam) (Al-Tamimi et al., 2011). Based on theses results, using shorter CFRP plate that covers 25% of the shear span of RC beams is sufficient and cost effective.

5.5 Effect of the Width of Prestressed CFRP Plate

The contribution of prestressed CFRP plate's width were studied in this thesis due to its reported major role in increasing strengthening capacity of the beams (Obaidat, 2011) . The load deflection curve for various widths of prestressed CFRP plate on strengthening RC beam are presented on Table 5.4. For strengthening by 5% prestressed CFRP plate, increasing the width of the CFRP plate by 40% (from 25 mm to 35 mm) increased both the yield and ultimate load by 0.97%, and 18.4%, respectively. On the other hand, decreasing the width by 66.67% (from 25 mm to 15 mm) reduced by 1.3%, and 6.58% for both the yield and ultimate loads, respectively. For retrofitting by 20% prestressed CFRP plate, increasing the width of the CFRP plate by 40% (from 25 mm to 35 mm) improved both the yield and ultimate load by 1.36%, and 19.3%, respectively. Conversely, reducing the width by 66.67% (from 25 mm to 15 mm) decreased by 1.42%, and 7.1% for both the yield and ultimate loads, respectively. For strengthening by 30% prestressed CFRP plate, increasing the width of the CFRP plate by 40% (from 25 mm to 35 mm) increased both the yield and ultimate load by 0.97%, and 18.4%, respectively. In contrast, decreasing the width by 66.67% (from 25 mm to 15 mm) decreased both the yield and ultimate loads by 1.3%, and 6.58%, respectively. Figure 5.5 shows the load-deflection curves for the effect of various widths for 5%

prestressed CFRP plate on strengthening RC beam. Based on the results, increasing the width of the prestressed CFRP plate to 35 mm delayed the debonding and the deflection occurred at 195.8 mm, while reducing the width of prestressed CFRP plate to 15 mm accelerated the debonding and deflected at 65.9 mm. According to the results, increasing the width of the CFRP plate has an influence on the flexural behaviour of retrofitted RC beam especially on the ultimate loads carrying capacity and delay in the debonding (almost 2.6 times of regular width). Primarily this effect is due to the additional resistance obtained by wider width of prestressed CFRP plate which increased the resistance to the shear stress developed on the contact between RC beam and CFRP plate (Obaidat, 2011).

Table 5.4 Effect of various width of CFRP plate

Prestressing Level (%)	Width of CFRP Plate (mm)	Yield Load (KN)	Increase/Decrease in Strength (%)	Ultimate Load (KN)	Increase/Decrease in Strength (%)
5	15	272.35	-1.3	291.8	-6.58
	25	275.8	-	311	-
	35	278.5	+0.97	368.4	+18.4
20	15	275.3	-1.42	294.1	-7.1
	25	279.2	-	315	-
	35	283	+1.36	378.4	+19.3
30	15	275.6	-1.53	298.9	-6.15
	25	279.83	-	317.28	-
	35	287.2	2.63	394	+25

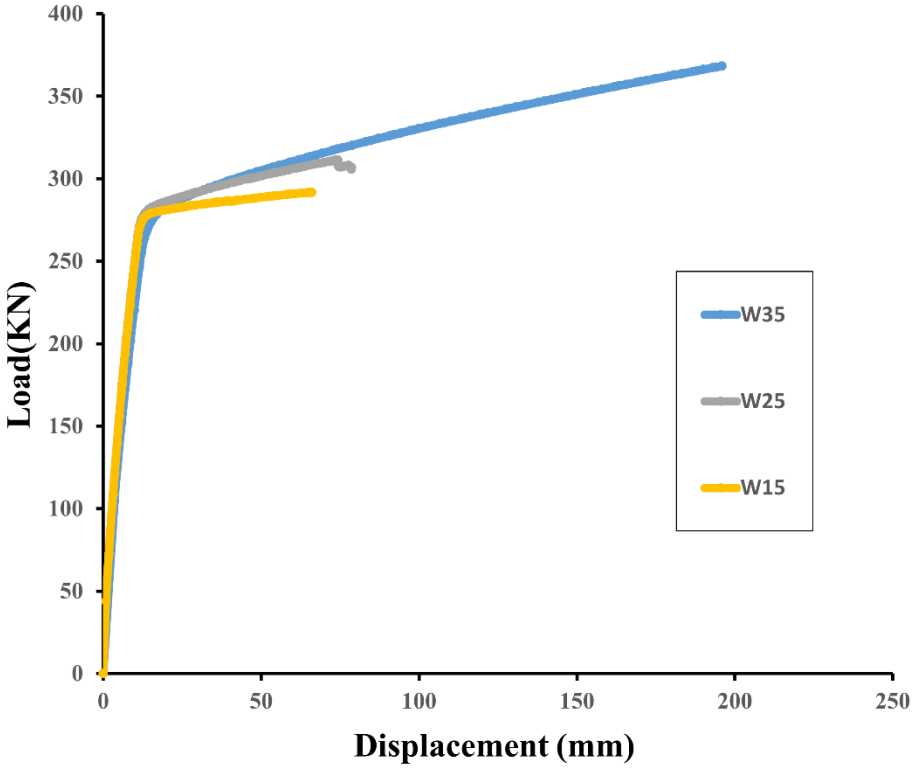

Figure 5.5 Effect of Various width of 5% prestressed CFRP plate.

5.6 Effect of the Thickness of Prestressed CFRP Plate

The contribution of prestressed CFRP plate's thickness was investigated in the parametric study, and there was a study conducted on this parameter (Obaidat, 2011) . The load deflection curve for various thicknesses of prestressed CFRP plate on strengthening RC beam are presented in Table 5.5. For retrofitting by 5% prestressed CFRP plate, increasing the thickness of the CFRP plate from 2 mm to 3 mm increased both the yield and ultimate load by 0.98%, and 6.56%, respectively. On the other hand, decreasing the thickness from 2 mm to 1 mm reduced both the yield and ultimate loads by 0.22%, and 6.73%, respectively. For strengthening by 20% prestressed CFRP plate, enhancing the thickness of the CFRP plate from 2 mm to 3 mm increased both the

yield and ultimate load by 0.32%, and 8.25%, respectively. Conversely, reducing the thickness from 2 mm to 1 mm decreased by 1.2%, and 7.21% for both the yield and ultimate loads, respectively. For strengthening by 30% prestressed CFRP plate, enhancing the thickness of the CFRP plate from 2 mm to 3 mm improved both the yield and ultimate load by 2.63%, and 8.42%, respectively. In contrast, decreasing the thickness from 2 mm to 1 mm decreased both the yield and ultimate loads by 0.66%, and 5.76%, respectively. Figure 5.6 shows the load-deflection curves for the effect of various thickness for 5% prestressed CFRP plate on retrofitting RC beam.

Table 5.5 Effect of various thickness of CFRP plate

Prestressing Level (%)	Depth of CFRP Plate (mm)	Yield Load (KN)	Increase/Decrease in Strength (%)	Ultimate Load (KN)	Increase/Decrease in Strength (%)
5	1	275.1	-0.22	291.4	-6.73
	2	275.8	-	311	-
	3	278.5	+0.98	331.4	+6.56
20	1	275.9	-1.2	293.8	-7.21
	2	279.2	-	315	-
	3	280.1	+0.32	341	+8.25
30	1	278	-0.66	300	-5.76
	2	279.83	-	317.28	-
	3	287.2	2.63	344	+8.42

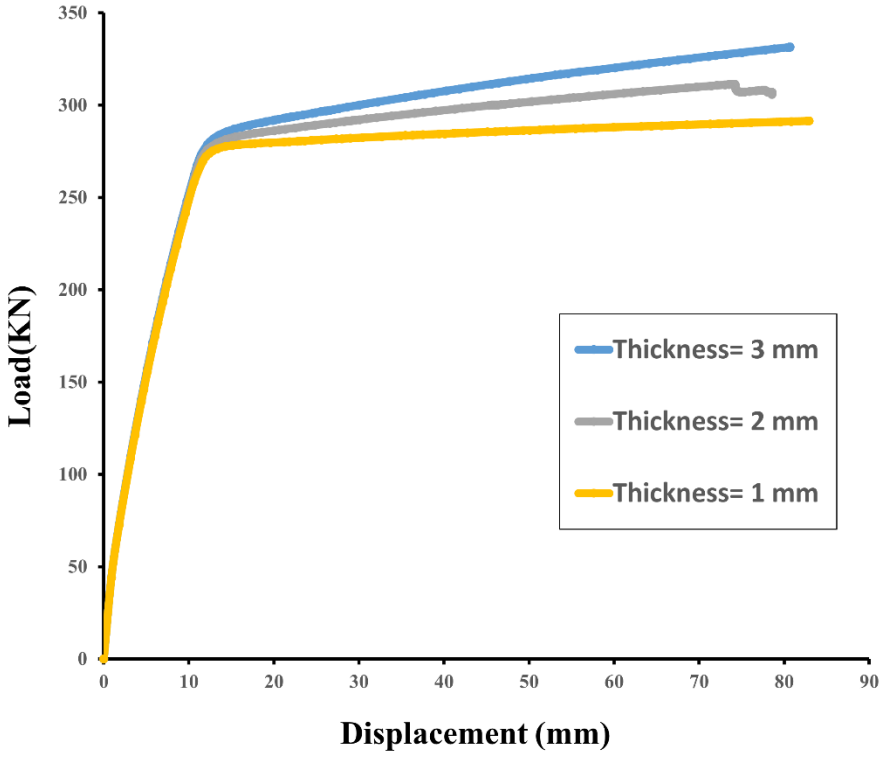

Figure 5.6 Effect of various thickness of 5% prestressed CFRP plate

According to the results, increasing the thickness of the CFRP plate has an influence on the flexural behaviour of retrofitted RC beam especially on the ultimate loads carrying capacity and almost no effect on delaying the debonding of CFRP plate. Primarily this is because of the same contact area between CFRP plate and RC beam (Obaidat, 2011).

5.7 Conclusion

The conducted parametric studies provided a comprehensive understanding on strengthening RC beam by prestressing CFRP plate. Prestressing of CFRP improves the strength of RC beam especially for the ultimate load. However, as the prestressing increased the mode of failure changed to rupture of the CFRP plate instead of debonding. This rupture occurred early with each increase of prestressing levels. The effect of using higher grades of steel reinforcement provided the retrofitted RC beam with prestressed CFRP plate with improvement in both the yield and ultimate loads. Therefore, using higher grade steel reinforcement will reduce the prestressing levels. Reducing the length of the CFRP plate reduced the yield and ultimate loads by 0.4% and 4.5%, respectively. The effect of various width of CFRP plate significantly affected the load carrying capacity of retrofitted RC beam, especially the ultimate load. Increasing the width of prestressed CFRP plate considerably improved the yield load by 1.3%, and ultimate load by 20% this was mainly by increasing the shear strength at the interfacial surface between CFRP plate and RC beam. On the other hand, reducing the width of prestressed CFRP plate reduced the load carrying capacity especially for the ultimate load because narrower width reduced the shear strength at bonding area between CFRP plate and RC beam and causing the debonding to occur earlier. Moreover, using thicker prestressed CFRP plate improved the flexural behaviour of retrofitted RC beams, especially on the ultimate load. Increasing CFRP plate's depth developed the yield load by 0.98%, and ultimate load by 6%. On the contrary, reducing the prestressed CFRP plate decreased the yield load by -0.61%, and ultimate loads by 6%.

Chapter 6: Conclusions and Recommendations

6.1 Introduction

The use of a prestressing FRP plate has become a common and attractive strengthening technique for retrofitting the RC beams due to its impact on reducing the stress in the concrete and steel reinforcement. Prestressing of the CFRP plate significantly improves the flexural behaviour of RC beams. Developing a FE model that simulates the flexural behaviour of RC beam strengthened with different prestressing levels of CFRP plate can provide a deeper understanding of the strengthening characteristics. The ABAQUS FE Package was used to develop and validate an RC beam model. A concrete damage plasticity model was applied to model the concrete behaviour and compare it with the experimental data in terms of load-deflection curve, failure mode, and crack patterns. After validating the FE model, parametric studies were conducted to investigate the effect of various prestressing levels of the CFRP plate, steel strength, CFRP plates' length, width, and thickness. The FE model can be considered for future study and design of RC beams strengthened with prestressed CFRP plate since it offers a reasonable representation of the experimental results for load-deflection curve, failure mode and crack patterns.

6.2 Conclusions

The proposed FE model was created and validated based on experimental behaviour. Some conclusions can be made as follows:

- The employed concrete damage plasticity model was appropriate to represent the RC beam strengthened with prestressed CFRP plate.
- 3D solid elements were suitable to represent the concrete behaviour.

- Truss elements were suitable to represent the main and transfer steel reinforcement and were considered as elastic perfectly plastic for the materials model.
- Shell elements were appropriate to represent the CFRP plate behaviour, and as simplification the CFRP plate was modeled as isotropic (not as orthotropic) because the load is applied in the axial direction of the CRFP plate.
- The perfect contact model between the concrete and internal steel reinforcement was a reasonable approximation of the reinforcement-concrete interface.
- A contact surface was used to represent the bonding between the RC beam and CFRP plate using a traction separation law, and it showed a good agreement with experimental findings.
- Displacement-controlled loading was able to represent the flexural behaviour of the RC beam strengthened with prestressed CFRP plate.
- Increasing prestressing level showed a significant influence only on the ultimate load.
- Increasing the steel strengths increased both the yield and ultimate loads.
- The length of the CFRP plate played a critical role in determining the ultimate load.
- Increasing the width of the CFRP plate improved the ultimate load and delayed debonding by increasing the bonding area between the CFRP plate and concrete.
- The thickness of the CFRP plate had a considerable impact on the ultimate load only and it has no influence on the failure mode because the contact area is the same.

6.3 Recommendations

The presented research contributes to improve understanding of flexural behaviour of RC beams strengthened with prestressed CFRP plate. It also provides information about selecting appropriate parts, materials properties, and understanding the necessity of bonding model between

the CFRP and concrete parts. Nevertheless, several investigations are recommended as future work.

The developed FE model can be used in designing any future experimental test regarding RC beam retrofitted by prestressed CFRP plate. Further investigation on the environmental effects on the materials properties of CFRP plate, concrete, and bonding model is recommended since it has a direct influence on the flexural behaviour and bonding properties. Also, additional work is needed to explore the effectiveness of different type of bonding materials due to its effect on the mode of failure of CFRP plate. Furthermore, in the concrete model, the damage parameters in compression and tension need further investigation.

Bibliography

ABAQUS (2011). “Theory Manual, and User Manual Version 6.11”. Dassault Systems Simulia Corp,

Providence, RI.

Abuodeh, O. R., Abdalla, J. A., & Hawileh, R. A. (2020). Prediction of shear strength and behavior of RC beams strengthened with externally bonded FRP sheets using machine learning techniques. *Composite Structures*, *234*, 111698.

ACI 440.R1-06., (2006). “Guide for the Design and Construction of Structural Concrete Reinforced with

FRP Bars”. ACI 440.IR-06.

ADINA R & D Inc. Theory and modeling guide. Watertown (MA, USA): ADINA R & D 2002.

ANSYS. ANSYS workbench documentation. Version 11. Canonsburg (PA): ANSYS Inc.; 2007.

Al-Tamimi, A. K., Hawileh, R., Abdalla, J., & Rasheed, H. A. (2011). Effects of ratio of CFRP plate length to shear span and end anchorage on flexural behavior of SCC RC beams. *Journal of Composites for Construction*, *15*(6), 908–919.

Aram, M. R., Czaderski, C., & Motavalli, M. (2008). Debonding failure modes of flexural FRP-strengthened RC beams. *Composites Part B: Engineering*, *39*(5), 826–841. https://doi.org/10.1016/j.compositesb.2007.10.006

Azam, A. (2015). *Numerical Modelling of Reinforced Concrete Walls Encased in Polyvinyl Chloride Stay-in-place Formwork*.

Badawi, M., & Soudki, K. (2009). Flexural strengthening of RC beams with prestressed NSM CFRP rods–experimental and analytical investigation. *Construction and Building Materials*, *23*(10), 3292–3300.

Brena, S. F., Bramblett, R. M., Wood, S. L., & Kreger, M. E. (2003). Increasing flexural capacity of reinforced concrete beams using carbon fibre-reinforced polymer composites. *Structural Journal*, *100*(1), 36–46.

Burlayenko, V. N., & Sadowski, T. (2008). FE modeling of delamination growth in interlaminar fracture specimens. *Budownictwo i Architektura*, *2*, 95–109.

Chaallal, O., Mofidi, A., Benmokrane, B., & Neale, K. (2011). Embedded through-section FRP rod method for shear strengthening of RC beams: Performance and comparison with existing techniques. *Journal of Composites for Construction*, *15*(3), 374–383.

Coronado, C. A., & Lopez, M. M. (2010). Numerical modeling of concrete-FRP debonding using a crack band approach. *Journal of Composites for Construction*, *14*(1), 11–21.

Cosenza, E., Manfredi, G., & Realfonzo, R. (1997). Behavior and modeling of bond of FRP rebars to concrete. *Journal of Composites for Construction*, *1*(2), 40–51.

de Domenico, D., Pisano, A. A., & Fuschi, P. (2014). A FE-based limit analysis approach for concrete elements reinforced with FRP bars. *Composite Structures*, *107*, 594–603.

de Lorenzis, L., & Teng, J.-G. (2007). Near-surface mounted FRP reinforcement: An emerging technique for strengthening structures. *Composites Part B: Engineering*, *38*(2), 119–143.

Demin, W., & Fukang, H. (2017). Investigation for plastic damage constitutive models of the concrete material. *Procedia Engineering*, *210*, 71–78. https://doi.org/10.1016/j.proeng.2017.11.050

Diab, H., & Wu, Z. (2007). Nonlinear constitutive model for time-dependent behavior of FRP-concrete interface. *Composites Science and Technology*, *67*(11–12), 2323–2333.

Dias, S. J. E., & Barros, J. A. O. (2013). Shear strengthening of RC beams with NSM CFRP laminates: Experimental research and analytical formulation. *Composite Structures*, *99*, 477–490.

Ebead, U. A., & Marzouk, H. (2005). Tension-stiffening model for FRP-strenghened RC concrete two-way slabs. *Materials and Structures*, *38*(2), 193–200.

El-Hacha, R., & Rizkalla, S. H. (2004). Near-surface-mounted fibre-reinforced polymer reinforcements for flexural strengthening of concrete structures. *Structural Journal*, *101*(5), 717–726.

Esfahani, M. R., Kianoush, M. R., & Tajari, A. R. (2007). Flexural behaviour of reinforced concrete beams strengthened by CFRP sheets. *Engineering Structures*, *29*(10), 2428–2444.

Garden, H. N., & Hollaway, L. C. (1998). An experimental study of the influence of plate end anchorage of carbon fibre composite plates used to strengthen reinforced concrete beams. *Composite Structures*, *42*(2), 175–188.

Genikomsou, A. (2015). *Nonlinear Finite Element Analysis of Punching Shear of Reinforced Concrete Slab-Column Connections*.

Godat, A., Chaallal, O., & Neale, K. W. (2013). Nonlinear finite element models for the embedded through-section FRP shear-strengthening method. *Computers & Structures*, *119*, 12–22.

Hajihashemi, A., Mostofinejad, D., & Azhari, M. (2011). Investigation of RC beams strengthened with prestressed NSM CFRP laminates. *Journal of Composites for Construction*, *15*(6), 887–895.

Hawileh, R. A. (2012). Nonlinear finite element modeling of RC beams strengthened with NSM FRP rods. *Construction and Building Materials*, *27*(1), 461–471.

Hawileh, R. A., Abdalla, J. A., Tanarslan, M. H., & Naser, M. Z. (2011). Modeling of nonlinear cyclic response of shear-deficient RC T-beams strengthened with side bonded CFRP fabric strips. *Computers & Concrete*, *8*(3), 193–206.

Hawileh, R. A., Naser, M. Z., & Abdalla, J. A. (2013). Finite element simulation of reinforced concrete beams externally strengthened with short-length CFRP plates. *Composites Part B: Engineering*, *45*(1), 1722–1730.

Hu, H. T., Lin, F. M., & Jan, Y. Y. (2004). Nonlinear finite element analysis of reinforced concrete beams strengthened by fibre-reinforced plastics. *Composite Structures*, *63*(3–4), 271–281. https://doi.org/10.1016/S0263-8223(03)00174-0

Krour, B., Bernard, F., & Tounsi, A. (2013). Fibres orientation optimization for concrete beam strengthened with a CFRP bonded plate: A coupled analytical–numerical investigation. *Engineering Structures*, *56*, 218–227.

Lou, T., Lopes, S. M. R., & Lopes, A. v. (2016). Response of continuous concrete beams internally prestressed with unbonded FRP and steel tendons. *Composite Structures*, *154*, 92–105.

Ma, C., Awang, A. Z., Garcia, R., Omar, W., & Pilakoutas, K. (2016). Behaviour of over-reinforced high-strength concrete beams confined with post-tensioned steel straps–an experimental investigation. *Structural Concrete*, *17*(5), 768–777.

Matta, F., Nanni, A., Abdelrazaq, A., Gremel, D., & Koch, R. (2009). Externally post-tensioned carbon FRP bar system for deflection control. *Construction and Building Materials*, *23*(4), 1628–1639.

Mercan, B., Schultz, A. E., & Stolarski, H. K. (2010). Finite element modeling of prestressed concrete spandrel beams. *Engineering Structures*, *32*(9), 2804–2813. https://doi.org/10.1016/j.engstruct.2010.04.049

Mitchell, D., & Collins, M. P. (1978). Influence of prestressing on torsional response of concrete beams. *PCI JOURNAL*, *23*(3), 54–73.

Nie, J., Wang, Y., & Cai, C. S. (2011). Experimental research on fatigue behavior of RC beams strengthened with steel plate-concrete composite technique. *Journal of Structural Engineering*, *137*(7), 772–781.

Obaidat, Y. T. (2011). *Structural retrofitting of concrete beams using FRP : debonding issues*. Department of Construction Sciences, Structural Mechanics, Lund University.

Obaidat, Y. T., Heyden, S., & Dahlblom, O. (2010). The effect of CFRP and CFRP/concrete interface models when modelling retrofitted RC beams with FEM. *Composite Structures*, *92*(6), 1391–1398.

Peng, H., Zhang, J., Shang, S., Liu, Y., & Cai, C. S. (2016). Experimental study of flexural fatigue performance of reinforced concrete beams strengthened with prestressed CFRP plates. *Engineering Structures*, *127*, 62–72.

Reddy, J. N. (2003). *Mechanics of laminated composite plates and shells: theory and analysis*. CRC press.

Rezazadeh, M., Cholostiakow, S., Kotynia, R., & Barros, J. (2016). Exploring new NSM reinforcements for the flexural strengthening of RC beams: Experimental and numerical research. *Composite Structures*, *141*, 132–145.

Smith, S. T., & Teng, J. G. (2002). FRP-strengthened RC beams. I: review of debonding strength models. *Engineering Structures*, *24*(4), 385–395.

Tavio, Anggraini, R., Raka, I. G. P., & Agustiar. (2018). Tensile strength/yield strength (TS/YS) ratios of high-strength steel (HSS) reinforcing bars. *AIP Conference Proceedings*, *1964*. https://doi.org/10.1063/1.5038318

Toutanji, H. A., & Gomez, W. (1997). Durability characteristics of concrete beams externally bonded with FRP composite sheets. *Cement and Concrete Composites*, *19*(4), 351–358.

van den Einde, L., Zhao, L., & Seible, F. (2003). Use of FRP composites in civil structural applications. *Construction and Building Materials*, *17*(6–7), 389–403.

Yang, D.-S., Park, S.-K., & Neale, K. W. (2009). Flexural behaviour of reinforced concrete beams strengthened with prestressed carbon composites. *Composite Structures*, *88*(4), 497–508.

Ye, L., Yue, Q., Zhao, S., & Li, Q. (2002). Shear strength of reinforced concrete columns strengthened with carbon-fibre-reinforced plastic sheet. *Journal of Structural Engineering*, *128*(12), 1527–1534.

Zhao, X. G., & Cai, M. (2010). A mobilized dilation angle model for rocks. *International Journal of Rock Mechanics and Mining Sciences*, *47*(3), 368–384. https://doi.org/10.1016/j.ijrmms.2009.12.007